



DEVELOPMENT AND VALIDATION OF A MODIFIED H-FLUME FOR ACCURATE FLOW MEASUREMENT IN RECTANGULAR CHANNELS

ACHOUR B.^{1}, AMARA L.², KULKARNI K.H.³*

¹ Professor, Research laboratory in subterranean and surface hydraulics (LARHYSS),
University of Biskra, Algeria

² Associate Professor, Department of Civil Engineering and Hydraulics, Faculty of
Science and Technology, University of Jijel, Algeria

³ Associate Professor, Department of Civil Engineering, Dr Vishwanath Karad MIT
World Peace University, Pune, India

(* *bachir.achour@larhyss.net*)

Research Article – Available at <http://larhyss.net/ojs/index.php/larhyss/index>
Received January 20, 2024, Received in revised form March 2, 2025, Accepted March 4, 2025

ABSTRACT

The study aimed to examine, from theoretical and experimental perspectives, the modified H-Flume as a flow measurement device for rectangular open channels. By introducing a vertical V-notch at the terminal section, the modified H-Flume allows for the derivation of theoretical relationship governing the discharge coefficient (C_d) and the stage-discharge relationship, overcoming the limitations of the original design. These relationships depend on the dimensionless parameter $M_1 = mh_1/B$, which encapsulates the key geometric and flow characteristics of the device.

Solely depending on M_1 , the study introduces the relative upstream flow depth h_1^* , which is a dimensionless parameter defined as the ratio of the upstream flow depth (h_1) to the critical flow depth ($h_{2,c}$) at the V-notch, capturing the hydraulic state of the upstream flow relative to critical conditions. This dimensionless parameter plays a pivotal role in determining the discharge coefficient (C_d). Indeed, the discharge coefficient (C_d) is fundamentally governed by h_1^* , as it encapsulates the energy transformation and flow behavior from the upstream subcritical state to the downstream critical state. This relationship ensures that C_d is a precise function of the hydraulic conditions at the approach channel and the geometry of the V-notch. The relationship between h_1^* and C_d is mathematically linked through energy principles and dimensionless parameters, emphasizing their interdependence. In addition, since C_d is directly influenced by h_1^* , the flow rate (Q) can be uniquely determined by measuring the upstream depth h_1 . This dependency eliminates ambiguity in the stage-discharge relationship and enables accurate

flow rate predictions. As practical implications, the explicit dependence of C_d on $h_1^*(M_1)$ simplifies flow measurements, as a single depth reading at the upstream section suffices to determine the discharge. This relationship enhances the practicality of the modified H-Flume, ensuring reliability across a broad range of flow conditions.

An increase in h_1^* corresponds to changes in flow dynamics and directly affects C_d , enabling the accurate estimation of the discharge rate (Q).

Explicit approximate equations for $h_1^*(M_1)$ were developed, simplifying the calculation of C_d while maintaining remarkable accuracy. These equations revealed that h_1^* is a critical intermediary variable, as it reflects the flow's evolution through the flume and its approach to the critical state at the V-notch. This link establishes the modified H-Flume as a semi-modular device where C_d depends not only on the geometric characteristics of the flume but also on the upstream flow conditions represented by h_1^* .

The strong theoretical and experimental foundation of this study confirms the reliability and practicality of the modified H-Flume. The established relationships between h_1^* , C_d , and Q offer a robust framework for precise flow measurement, providing significant advancements in open-channel hydraulics. This makes the modified H-Flume an invaluable tool for applications requiring high accuracy and versatility across a wide range of flow conditions. Indeed, four modified H-Flumes, with varying geometries, were subjected to experimental testing across 1480 flow conditions. Results show excellent agreement between theoretical and experimental discharge coefficients, with maximum deviations of only 0.185%. This validates the modified H-Flume's accuracy and reliability, making it a practical and theoretically sound tool for open-channel flow measurement.

Keywords: Modified H-Flume, Flow Measurement, Discharge Coefficient, Discharge, V-notch, Open Channel Hydraulics, Rectangular channel, Semi-modularity.

INTRODUCTION

The measurement of flow in open channels and pipes has historically posed a significant challenge in hydraulics, shaping the development of gauging methodologies that combine theoretical rigor with practical applicability. These methodologies aim to reliably quantify discharge, a cornerstone for water resource management, irrigation systems, and hydraulic engineering.

Among the diverse array of flow measurement devices, weirs have emerged as a cornerstone due to their ability to utilize the principles of free-spilling flow. These structures, characterized by their distinct geometric configurations, create predictable hydraulic conditions that facilitate accurate discharge estimation. Weirs are categorized by their crest profiles, which can include thin vertical plates or incorporate notches of various shapes, such as V-notch, rectangular, or parabolic. Each design serves a specific purpose. V-notch weir, known as the Thomson weir, excels in sensitivity to low flow rates. Indeed, it is renowned for its exceptional accuracy in measuring upstream flow

depth. Its triangular geometry inherently amplifies the precision of depth readings, particularly for low and high flow rates, making it the preferred choice for applications requiring minimal deviation in discharge calculations.

In contrast, sharp-crested rectangular weirs, while historically significant, exhibit reduced precision under low flow conditions. This limitation arises primarily from their susceptibility to lateral contraction effects, which distort the flow profile and introduce measurement inaccuracies, as highlighted in foundational studies by Bazin (1898), SIA (1926), Kindsvater and Carter (1957), De Coursey and Blanchard (1970), Bos (1976), 1989), Achour et al. (2003), Achour and Amara (2021e), and subsequent research.

The evolution of weir technology has been driven by recent theoretical and experimental investigations aimed at refining the relationships that govern the discharge coefficient (C_d). These studies strive to enhance the predictive accuracy of discharge calculations, ensuring consistency with empirical data across varying flow conditions. For those seeking a comprehensive understanding on weirs with notches of common shapes, the following references, and others, provide foundational insights into the principles and advancements in weir technology (Achour and Amara, 2021a; 2021b; 2021c; 2021d; 2021e; Achour et al., 2022a; Achour et al., 2022b). These are modern studies systematically updated and validated the theoretical frameworks governing the discharge coefficients of various weirs. These efforts have aligned theoretical predictions with experimental observations, offering enhanced reliability in practical applications.

The choice of weir design directly impacts the accuracy and reliability of flow measurement. Weirs devoid of crest height are some of the best, with their self-cleaning geometry, mitigating sediment accumulation and ensuring consistent readings, making them indispensable in settings where precision is paramount. Meanwhile, rectangular weirs may remain suitable for applications where broader flow ranges take precedence over pinpoint accuracy.

It is reported in the literature the last advancements in flow measurement devices, particularly focusing on the circular thin-walled weir and the sharp-edged width constriction. Recent studies have highlighted significant developments in the modeling and analysis of circular thin-walled weirs working under free flow, and under partially submerged conditions. A novel approach has been proposed for modeling the discharge behavior of these devices. Notable contributions in this area include the works of Brandes and Barlow (2012), Vatankhah and Bijankhan (2013), and Achour and Amara (2021d), who provided foundational insights into the behavior of such weirs.

Among various flow measurement tools, sharp-edged width constrictions stand out due to their simplicity, affordability, and ease of implementation. This device, devoid of crest height, comprises two vertical thin plates arranged transversely to the flow, forming a central opening of width b . This arrangement is recognized as one of the simplest devices ever designed for measuring open-channel flows. In contrast to trapezoidal-shaped openings, as studied by Farzad and Vatankhah (2023), the rectangular shape of sharp-edged constrictions facilitates a rigorous theoretical approach. As stated by Achour and Amara (2021f), this shape allows for the derivation of a discharge coefficient relationship

that accounts for the influence of approach flow velocity. Achour and Amara (2021f) have demonstrated that the theoretical discharge coefficient depends solely on the contraction rate ($\beta = b/B$), where B is the width of the rectangular approach channel. This dependency was predicted using dimensional analysis and subsequently confirmed through both theoretical and experimental studies. In addition, both dimensional and experimental analyses revealed that the relative upstream flow depth (h/B) in no way affects the discharge coefficient within the practical range of β . This finding simplifies the application of the device in various scenarios. The alignment between predicted and experimental discharge coefficients was notable, with a maximum deviation of less than 2%. Subsequent corrections based on experimental observations further reduced the deviation to 1.36%, demonstrating the high accuracy and reliability of the theoretical model.

The study conducted by Achour and Amara (2025, in press) presents a theoretical and experimental analysis of sharp-edged width constrictions with rectangular central openings in open trapezoidal-shaped channels. The research focuses on establishing the effectiveness of these constrictions as flow measurement tools. The study employed two well-established energy principles to derive the governing discharge coefficient relationship. These theories yielded identical results, confirming the robustness of the approach. The research demonstrated that the discharge coefficient depends exclusively on two parameters, namely, the contraction rate of the device, and the non-dimensional parameter mh_1/b , where m = Side slope of the trapezoidal approach channel, h_1 = Upstream water depth, and b = Base width the trapezoidal approach channel. The study included 1,012 measurement points, covering a broad range of flow conditions. The experimental results closely matched theoretical predictions, demonstrating the validity of the proposed model. The maximum deviation between theoretical predictions and experimental observations was only 0.3%. This exceptionally low error margin confirms the high reliability and accuracy of the theoretical discharge coefficient relationship. The study confirms that sharp-edged constrictions with rectangular openings can serve as precise flow measurement devices in trapezoidal channels. This research provides a practical tool for trapezoidal open-channel flow measurement, useful in irrigation systems, hydraulic engineering projects, and environmental flow monitoring. The robust theoretical foundation ensures reliable flow rate predictions, reducing the need for empirical calibrations.

In recent years, innovative flow measurement tools have been analyzed from both theoretical and experimental perspectives to establish the stage-discharge relationship. These devices include broad-crested weirs, available in triangular or rectangular configurations, with or without crest heights.

Thin-crested and broad-crested weirs continue to be of significant practical value in numerous hydraulic structures. Their adaptability and utility make them essential tools in flow measurement applications.

To explore the latest advancements in the design and application of these weirs, the literature provides an extensive list of key references. Recent notable works include those by Achour and Amara (2020, 2022a, 2022d, 2022e, 2023), Kulkarni and Hinge (2021,

2023), and collaborative studies by Achour et al. (2022b, 2022c). Kulkarni and Hinge's articles focused on advancements in discharge measurement techniques using compound broad-crested weirs and the application of additive manufacturing for performance enhancement.

Weirs with longitudinal triangular-profile, such as the Bazin and Crump weirs, are recognized for their use in measuring flow rates in open channels. Despite their similar shapes, these weirs differ in the upstream and downstream slope values they employ. Bazin weir incorporates four combinations of upstream and downstream slopes, offering greater variability in design (Bazin, 1898). Crump simplified the design to a single slope combination of 1:2 upstream and 1:5 downstream, making it more straightforward to implement (Henderson, 1966; Bos, 1976; Hager, 1986; Achour et al., 2003). Both Bazin and Crump weirs are constrained in their application, as they are primarily suited for rectangular open-channel flow measurements, limiting their versatility. In addition, Bazin's weir failed to achieve widespread adoption due to its calibration for a large crest height ($P = 50$ cm), which was impractical for industrial channels of the era (Afblb, 1970). This design flaw has not been revisited or corrected in subsequent studies.

The latest advancements in the study of Crump weirs are documented in the works of Zuikov (2017) and Achour and Amara (2022f). These studies focus on refining the understanding of the stage-discharge relationship, a key factor in flow measurement. Zuikov's research derived a stage-discharge relationship that contributed significantly to the field of flowmetry, despite a deviation of almost 5% in the flow rate calculation. However, it was later determined to be incomplete. Achour and Amara (2022f) identified a critical oversight in Zuikov's model—the omission of the relative upstream flow depth (h/B), where h is the flow depth above the weir crest and B is the width of the rectangular approach channel. Their findings showed that h/B influences the discharge coefficient (C_d) by an average of 23.5%. Achour and Amara developed a new stage-discharge relationship that incorporates the h/B parameter. This model achieved a remarkable maximum deviation of only 0.864% in the computation of both the discharge coefficient (C_d) and the flow rate (Q) under free overflow conditions. The revised relationship proposed by Achour and Amara (2022f) is considered the most accurate and comprehensive C_d relationship ever developed for Crump weirs, making it a pivotal contribution to hydraulic engineering.

Achour and Amara (2023) recently introduced the "2A triangular weir," a triangular-shaped longitudinal profile weir named to honor its creators. This weir has undergone extensive studies involving design, theoretical modeling, and experimentation. The upstream and downstream slope values of the "2A triangular weir" are identical to those of the Crump weir. This design choice was driven by hydraulic imperatives, such as ensuring perfect flow adhesion to the weir's walls and enhancing its efficiency. Unlike the Crump and Bazin weirs, which rely on rectangular cross-sections, the "2A triangular weir" is composed entirely of triangular cross-sections, whose advantageous properties in flowmetry are universally recognized. In addition, this design grants it a universal range, making it suitable for flow measurement in all known open channel shapes. The triangular cross-section of the "2A triangular weir" allows for more precise readings of upstream depths and accurate discharge estimations. Moreover, its design eliminates

transitions between the device and the channel walls, ensuring that the discharge coefficient remains unaffected by the relative upstream depth (h/B), a limitation seen in the Crump weir. The "2A triangular weir" is classified as a semi-modular device. Its flow rate is influenced by both its geometric characteristics and the height of the water sheet above the crest, as confirmed by Achour and Amara's research.

Flumes, well-known hydraulic devices, have been widely used for measuring open channel flow. These structures are specifically designed to control, direct, and measure water flow in various applications, including hydrological studies, irrigation systems, wastewater treatment, and overall water resource management. The primary function of a flume is to provide an environment where the flow rate can be accurately gauged and manipulated. Flumes are typically constructed with specific shapes, such as parabolic, trapezoidal, or V-shaped cross-sections. These shapes help in directing and controlling the water flow efficiently. When properly designed and installed, flumes ensure a stable and uniform flow profile, which is essential for achieving precise flow measurements.

The flow rate within a flume is usually determined by correlating the water depth at a specific location with pre-established empirical formulas. These formulas take into account various factors, including the flume's geometry, the upstream water depth, and the flow characteristics. Furthermore, flumes are often incorporated into water management systems to regulate flow rates, ensuring that water is delivered in controlled quantities without excessive loss due to turbulence or uncontrolled flow. Flumes are generally simple in construction but designed to be highly durable. They are commonly made from materials such as concrete, steel, or masonry, which ensure long-term reliability under varying flow conditions. The robustness of these materials guarantees that the flume functions effectively over extended periods, even when subjected to fluctuating hydraulic loads.

Several well-established flume types have been developed and studied over time. Some of the most recognized include Parshall Flume (1936) – A widely used flume for accurate flow measurement, Venturi Flume in its original and modified shapes (Bos, 1976; 1979; Achour et al., 2003; Hager, 1986) – Originally designed for improved accuracy in flow control, Trapezoidal Flume (Open Channel Flow, 2024) – Known for its efficiency in water flow regulation, the new Trapezoidal Flume, recently developed by a theoretical and experimental collaborative study (Achour et al., 2024) simple in form, easy to implement and with unmatched accuracy, Modified Monona Flume (Achour et al., 2024), a recently developed flume with enhanced performance, and H-Flume, a well-known flume that is being further modified for improved accuracy and control.

Since most of these flumes feature rectangular cross-sections, they often have limited accuracy in measuring low flow rates. To address this issue, Achour and De Lapray (2023) designed and tested a triangular cross-section flume that offers remarkable accuracy in calculating both high and low flow rates. This newly developed flume also has the added advantage of being self-cleaning due to its flat bottom, allowing for efficient passage of sediments and small debris, which can otherwise impact measurement precision. Readers will also find in the previously cited study how to design the device

based on equations derived from indisputable geometric considerations, including the relationship governing the transition.

In the present study, the authors investigate a modified version of the H-Flume from design, theoretical and experimental perspectives. This modified flume consists of two flat vertical walls forming a converging rectangular channel, which terminates in a vertical suppressed V-notch discharge without a crest height. A key characteristic of this design is its V-shaped discharge, which minimizes resistance to downstream submergence. Consequently, the flume exhibits small submergence ratios, not exceeding 25%, making it most suitable for free-spilling flow conditions. The unique shape of the proposed device allows for the derivation of a theoretical discharge coefficient and the corresponding stage-discharge relationship, thereby filling the gaps of the original H-Flume. It is worth noting that theoretical relationships are derived from fundamental principles (e.g., conservation laws, Newtonian mechanics, fluid dynamics), making them applicable across a broad range of conditions. In contrast, empirical relationships are often specific to the dataset or experimental conditions under which they were developed, limiting their applicability. In addition, theoretical models provide predictions based on governing equations and known physical laws, making them more accurate in untested conditions, while empirical models are curve-fitted to specific data points and may fail outside the tested range. Moreover, theoretical models explain why a particular phenomenon occurs, offering a deeper understanding of underlying mechanisms. Empirical models provide numerical correlations but do not necessarily explain why the relationship exists. Theoretical relationships can be modified or extended as new variables or conditions arise, while empirical relationships must be recalibrated or rederived if conditions change beyond their initial data set. Since theoretical models are derived from fundamental principles, as is the case in the present study, they remain valid across multiple scales (e.g., from laboratory to real-world applications), while empirical relationships are often scale-dependent and may not perform well when extrapolated. These are often affected by measurement errors, experimental limitations, or bias. In contrast, theoretical models rely on mathematical derivations and, when correctly applied, are free from experimental inaccuracies. As a general rule, while empirical relationships are valuable for practical applications where theoretical derivations are difficult, theoretical relationships offer greater universality, accuracy, scalability, and explanatory power. In hydraulic engineering and flow measurement, for instance, theoretical models allow for precise flow predictions without relying on limited experimental datasets.

Given the numerous advantages of theoretical relationships over empirical ones, it is strongly recommended that practitioners in the field of flow measurement prioritize devices that allow for theoretical development. Theoretical models provide greater accuracy, reliability, and adaptability, ensuring that measurement devices remain effective across various conditions. A notable example of such a device is the newly modified H-Flume, which has been designed based on theoretical principles. This practical and reliable solution enhances flow measurement applications by incorporating improved precision, reduced submergence effects, and optimal flow regulation.

By adopting devices with strong theoretical foundations, practitioners can benefit from greater predictive capabilities, scalability, and long-term usability, making them more efficient and adaptable to diverse hydraulic engineering applications.

ORIGINAL H-FLUME

The H-Flume is a specialized hydraulic structure used for measuring the flow rate of water in open channels and irrigation systems. It is particularly effective under low to moderate flow conditions, providing accurate measurements with minimal head loss. The design and operation of the H-Flume rely on precise geometric configurations, which enable flow rate calculations based on depth measurements at a specific location.

The H-Flume features a trapezoidal inclined notch, assumed as a terminal inclined V-notch cross-section, accompanied by vertical converging sidewalls and a flat base. Although the trapezoidal base width is relatively small compared to the overall dimensions of the device, an unusual assumption in existing literature is that this trapezoidal-shaped terminal cross-section is considered equivalent to a V-notch; to state that the terminal section of the H-Flume is triangular in shape is simply a misuse of language. From a purely geometric standpoint, this assumption appears unconventional, as a true V-notch cross-section was not directly adopted. Based on the authors' research, no documented photographic evidence or descriptive diagrams exist in the literature that depict an original H-Flume with a true V-notch terminal cross-section. The absence of such references raises questions about the geometric interpretation of the traditional H-Flume design. Moreover, adopting a true V-notch configuration could have facilitated theoretical flow development, whereas the trapezoidal cross-section does not offer the same advantage for deriving theoretical flow equations. In addition, assuming the terminal section of the H-Flume as of a triangular shape seems simplifying mathematical modeling while maintaining accuracy in discharge computations. Several hydraulic, geometric, and experimental factors justify this assimilation. Due to the small horizontal bottom width at the base of the exit section, the effective flow area resembles a triangular shape, making it reasonable to approximate it as such. The bottom width has a negligible effect on the flow acceleration at the notch, and the location of the control section. As a result, the flow behaves as if it were in a triangular cross-section, which validates the triangular assumption. In low-flow conditions, the flow may engage the entire trapezoidal section, but this effect is minor. A purely trapezoidal model would complicate calibration, requiring site-specific corrections. By approximating the exit section as triangular, engineers achieve: simplified discharge calculations, and consistent and reliable flow measurement. As a result, the triangular model is practically sufficient for engineering applications. Several studies and hydraulic handbooks have implicitly or explicitly confirmed that the trapezoidal terminal section of an H-Flume can be assimilated to a triangular section, such as the relevant study of Bos (1989). If the H-Flume terminal section were strictly trapezoidal, additional terms would need to be included in the stage-discharge relationship. The trapezoidal terminal section of the H-Flume is rightly assimilated to a triangular section, both for mathematical simplicity and practical

accuracy. Since experimental validation shows excellent agreement with the standard triangular form, the trapezoidal correction is unnecessary.

This assumption is well-supported in the literature, ensuring reliable and precise discharge measurement. However, despite the assimilation to a triangular section is reasonable, there is a need for further investigation into the geometric configuration of the H-Flume, particularly regarding the theoretical advantages of a true V-notch over the traditionally assumed trapezoidal section. A revised H-Flume design with a precisely defined V-notch could improve flow measurement accuracy and enable more robust theoretical modeling. However, the V-notch could cause: stronger contraction, causing higher flow velocities and potential instability, difficulty to maintain stable critical flow, affecting measurement accuracy, and higher risk of excessive turbulence and flow disturbances. May be, this is why hydraulic engineers seem preferring the trapezoidal outlet design in H-Flumes, causing moderate flow contraction, ensuring stable and predictable flow behavior, ensuring well-defined control section, allowing for accurate discharge measurement, more gradual velocity increase, preventing excessive turbulence.

Photos 1a and 1b depict an original H-Flume in operation, with one image showing field application and the other illustrating laboratory testing under free-spilling flow conditions. The H-Flume is positioned downstream of a rectangular approach channel, which conveys the flow to be measured. In the foreground, the inclined V-notch-like outlet section is clearly visible. This section is notable for its lack of a diverging section, a characteristic that influences flow behavior. The inclination of the terminal cross-section is a result of the bevelling of the vertical walls, yet the literature does not provide specific values for the bevel angle, leaving room for uncertainty in its geometric characterization.

The base width of the trapezoidal section in the H-Flume is a function of its overall dimensions, and its significance varies with the size of the device. Consider the following examples from Fiberglass H-Flumes: 0.75-foot depth H-Flume: Entry width: 43.43 cm, Base width: 2.29 cm; 1.0-foot depth H-Flume: Entry width: 57.91 cm, Base width: 3.05 cm; 4.5-foot depth H-Flume: Entry width: 260.60 cm, Base width: 13.72 cm.

From these values, it is evident that the base width is significantly smaller than the entry width. An important observation is that the base width of the trapezoidal section increases with the depth of the H-Flume. This relationship suggests that larger H-Flumes exhibit proportionally wider base sections, which may influence flow measurement accuracy and theoretical discharge formulations.

The absence of bevel angle specifications in the literature, combined with the uncertainty regarding the impact of the trapezoidal base width, indicates the need for further investigation. Specifically: 1) A geometric and hydraulic analysis is required to determine whether the trapezoidal cross-section can be approximated as a V-notch for flow measurement purposes, 2) Experimental studies and computational models could provide insights into the effect of the base width on flow characteristics and measurement accuracy. In other words, the observations presented emphasize the importance of precise geometric characterization in the design and theoretical modeling of the H-Flume. Future

studies should focus on quantifying the impact of the base width and determining whether the V-notch assumption is valid, particularly for practical hydraulic applications.



(a)



(b)

Photo 1: View of an original H-Flume, (a) in a field operation, (b) in laboratory testing. (Photos Open Channel flow, 2024)

In Photos 1a and 1b, the flat bottom of the H-Flume is clearly visible. This design feature contributes to its self-cleaning capability, meaning that the device effectively facilitates the passage of sediment and small debris. This property enhances its operational efficiency and minimizes maintenance needs, making it a practical choice for open channel flow measurement.

The H-Flume is not named after its geometric shape, as one might assume. Instead, the designation stems from the historical classification system used by researchers from the U.S. Soil Conservation Service. The letter "H" corresponds to the eighth letter of the alphabet, indicating that it was the eighth flume type studied in their series of hydraulic investigations.

In general, flow measurement devices should be designed in a manner that facilitates theoretical calculations, ensuring accuracy and reliability in practical applications.

The H-Flume is optimized for medium flow rates, with a maximum discharge capacity (Q) of 2.384 m³/s. Due to its relatively short length, the primary measurement point, denoted as H_a , is located near the device's inlet. This positioning is essential for capturing accurate water level readings, which are used to compute the flow rate using established hydraulic principles.

Since its conception in the mid-1930s, the original H-Flume has not been theoretically studied to derive a governing discharge coefficient (C_d) relationship, and consequently, a theoretical equation for the discharge (Q). The primary reason for this omission is likely the particular shape of the H-Flume, which makes theoretical derivations more complex compared to other flume types. Although the H-Flume design dates back several decades, its final dimensions and experimentally derived discharge relationships were not formalized until the late 1970s and even into the late 1980s. Notable studies contributing to this development include: Bos (1976), Gwinn and Parsons (1976), Brakensiek et al. (1979). Furthermore, the dimensions for the approach sections of the H-Flume were not specified until the mid-1980s (Gwinn, 1984). This late presentation of design specifications reinforces the notion that the H-Flume lacks a comprehensive theoretical model, making it a device that cannot be fully controlled using a single governing equation.

The flow rate (Q) in an original H-Flume is determined using an empirical flow equation tailored to the specific design of the H-Flume. This equation relates the measured head (H)—i.e., the water depth above a reference point—to the flow rate.

H-Flumes are specifically designed for measuring low to moderate flows in open channels. However, their flow rate equations are purely empirical, relying on calibrated experimental data. The geometry of the H-Flume, including its size, determines the constants used in the empirical equations, further limiting its theoretical generalization.

According to the literature, the original discharge equation for the H-Flume was not a single equation but instead consisted of three distinct equations for different flow regimes:

one for low flows, i.e., upstream depth varying within the following range $0.000109 \leq H$ (ft) < 0.001305, corresponding to $Q = 0.000109 - 0.001305H$ (ft), one for transitional flows, i.e. upstream depth varying within the following range $0.001305 \leq H$ (ft) < 1.5 corresponding to $Q = a + bH^{0.5} + cH^{2.5}$ where the value of the constants a , b , and c are tabulated depending on the H-Flume type and size (Open channel flow, 2024), and the third and last equation is for main flows, i.e., upstream depth varying within the following range $1.5 \leq H$ (ft) < 2.5 corresponding to $Q = 1.5 + 0.6645462H$ (ft). The presence of

multiple flow rate equations for different flow regimes makes the calculation process cumbersome and less practical for engineering applications. To address this complexity, Bos (1976) analyzed experimental flow rate and upstream depth values available in the literature (Open Channel Flow, 2024) and proposed a simplified, standardized equation. His equation provides an accuracy of within $\pm 3\%$, making it significantly more practical for field applications. It reads as follows:

$$\log Q = A + B \log H_a + C (\log H_a)^2 \quad (1)$$

Thus, the discharge equation for the H-Flume relies on tabulated constants A, B, and C, whose values are specifically dependent on the H-Flume depth (Open Channel Flow, 2024). The depth of the H-Flume typically ranges between 15.2 cm and 137 cm.

However, if the depth of a given H-Flume falls between two tabulated values, it becomes necessary to interpolate the constants, introducing potential inaccuracies in the flow rate calculation. As a result: 1) The relative error in calculating the discharge (Q) using the standard equation is likely greater than 3%, contradicting the claim by Bos (1976), 2) The accuracy of flow measurements can be compromised, particularly for depth values not explicitly provided in the tables.

This lack of precision highlights the empirical nature of the H-Flume discharge equation and raises concerns about its theoretical soundness.

It is reasonable to conclude that the existing discharge equation for the H-Flume lacks theoretical rigor. Specifically: 1) The form of the equation does not align with any established theoretical standards or governing principles in fluid mechanics, 2) Despite its empirical accuracy, it fails to meet the theoretical expectations typically required in the field of flow measurement, 3) The absence of a theoretically derived stage-discharge relationship makes the device less controllable compared to other flumes with well-defined governing equations. These limitations emphasize the need for a more theoretically sound approach to defining the discharge coefficient and flow rate relationships for the H-Flume.

Denoting D as the H-Flume depth, several geometric relationships are commonly used to define its following proportions: the average width of the device is approximately 1.90D, the short length of the H-Flume is typically 1.35D, approach section lengths have been investigated extensively by Gwinn (1984), who tested sections of varying the following lengths: 2.5D, 3.75D, 5D. His findings indicate that a 5D-long approach section provides the most accurate and reliable results. As a general standard, the length of the approach section is typically 3 to 5 times the maximum anticipated head (Hmax); by default, Hmax is assumed to be equivalent to the flume's depth (D). These dimensional considerations are crucial in ensuring the accuracy and efficiency of the H-Flume in practical field applications.

By way of compilation, while the H-Flume remains a widely used device for flow measurement in various fields, its empirical nature and lack of theoretical rigor present challenges. Future research should focus on:

- Developing a theoretically derived discharge equation to enhance its controllability and accuracy.
- Addressing the limitations of tabulated constants by proposing a continuous function that eliminates the need for interpolation.
- Investigating alternative geometric configurations that allow for theoretical stage-discharge relationships, improving the precision of flow measurements.

By addressing these challenges, the H-Flume could evolve into a more scientifically robust and reliable flow measurement device for modern hydrological and environmental applications.

MATERIAL AND METHODS

Description of the modified H-Flume and the resulting flow

Fig. 1 presents a plan view of the channel, illustrating the placement of the flow measuring device and the resulting longitudinal flow profile. The device is designed to measure flow rates by incorporating two vertical walls within a rectangular approach channel, forming a converging rectangular section that directs and accelerates the flow. The device consists of two primary sections: 1) Initial Rectangular Section (1-1) of width (B) matches the width of the rectangular approach channel. The flow depth at this section before entering the converging region is h_1 . 2) Exit Terminal Section (2-2) of vertical triangular-shaped section, devoid of crest height, where the flow depth denoted as $h_{2,c}$ indicating a critical flow condition (Fig. 2). The subscript "c" highlights that the flow is in a critical state at this location. As the flow enters the converging section, it experiences a restriction, leading to acceleration and a corresponding decrease in flow depth. Upon passing through the V-notch outlet, the flow transitions into a critical state, where the velocity reaches a maximum for the given depth. The V-notch outlet is defined by the top width (b) which is the narrowest width of the section, the total depth (h_0) of the approach channel, which also corresponds to the height of the device. The contraction rate (β) of the device is given by the ratio $\beta = b/B$. This ratio determines the extent of flow constriction, influencing the velocity and depth transitions through the device.

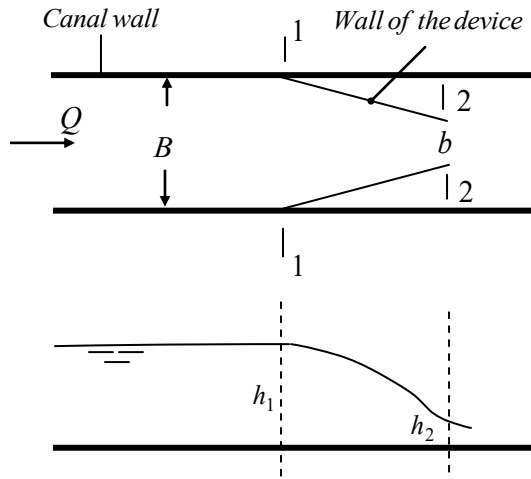
Thus, the flow measuring device operates based on a converging rectangular-to-triangular transition, ensuring that the flow reaches a critical state at the exit. Understanding the contraction ratio and flow acceleration is crucial for accurate discharge measurements. Future studies could focus on optimizing the contraction ratio (β) for improved flow measurement accuracy.

The modified H-Flume features a rectangular inlet section and a vertical triangular outlet section, making it an improved version of the conventional H-Flume. In contrast to the original H-Flume, which has an inclined V-notch outlet section formed by bevelling the vertical walls (as shown in Photo 1), this modification introduces a strictly defined V-notch at the exit. This structural enhancement leads to improved hydraulic performance.

Furthermore, the modified H-Flume can also be considered an improved version of the Montana Flume (Open Channel Flow, 2024; Achour et al., 2024), given its optimized outlet section. The modified H-Flume is anticipated to outperform the modified Montana Flume (Achour et al., 2024) due to the well-known advantages of V-notch configurations, including enhanced Flow Control with the V-notch design raising the upstream water level, facilitating more precise water level readings, Improved Accuracy with the integration of a V-notch ensuring high precision for both high and low flow rates, which is a critical aspect in flow measurement applications, Better Flow Regulation with the V-notch functioning as a control section, ensuring stable flow conditions and improved gauge readings.

As detailed in subsequent sections of this study, the modified H-Flume is a configuration that allows for theoretical development, making it a controllable flow measurement device. The introduction of a V-notch at the outlet enables the derivation of theoretical discharge relationships, enhancing the accuracy and predictability of flow rate calculations. For any flow measurement device to function correctly, the existence of a control section is a *sine qua non* condition. In the case of the modified H-Flume, this condition is met at the V-notch, where the flow reaches a critical state (Fig. 2). The presence of this critical flow section ensures that the flow rate is uniquely related to the upstream depth, enabling precise discharge calculations, and the device operates in a stable hydraulic regime, reducing uncertainties in flow measurement.

Summing up the above, the modified H-Flume, with its vertical triangular outlet and integrated V-notch, represents a significant improvement over both the traditional H-Flume and the modified Montana Flume. Its design allows for better flow regulation, improved measurement accuracy, and theoretical discharge derivations, making it a superior choice for hydraulic flow measurement applications.



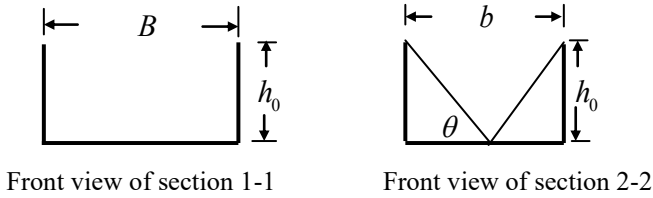


Figure 1: Plan view of the channel and the device as well as the longitudinal profile of the flow

Fig. 2 illustrates the flow characteristics within the modified H-Flume, which is installed in a rectangular approach channel designed to convey the discharge Q to be measured. The figure highlights key hydraulic parameters at different sections of the device.

It is observed that the total head (H_1) in the initial section (1-1) is equal to the critical total head (H_c) in the control section (2-2). This equivalence is justified by the assumption that pressure losses are negligible, given the short length of the device. Consequently, the energy balance remains unchanged between these two sections, and the flow acceleration and transition to critical conditions occur smoothly within the converging section.

The assumption of neglecting pressure drop simplifies the mathematical modeling of flow behavior in the device. This allows for the derivation of a stage-discharge relationship based on critical flow theory, accurate determination of flow rates using upstream water depth measurements, and enhanced predictability and control of the hydraulic conditions within the device.

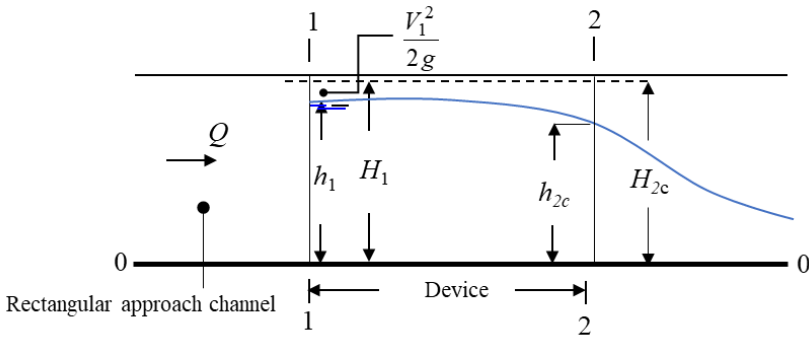


Figure 2: View of the longitudinal flow profile inside the authors' advocated modified H-Flume

Fig. 3 provides a perspective view of the designed portable modified H-Flume, highlighting its various structural components. One of the key elements of this design is the V-notch, which is: fixed to the device walls and bottom using rivets, constructed from a thin stainless steel metal plate with a thickness of just 1 mm, ensuring that it does not present any constructive constraints, and sealed using a rubber waterproof joint to ensure water tightness at the output section, preventing leakage and maintaining measurement accuracy.

These design choices contribute to the durability, portability, and efficiency of the modified H-Flume, making it a reliable solution for field applications.

To ensure optimal hydraulic performance, the authors recommend determining the length (L) of the device using the relationship governing the length of the modified Montana Flume, i.e., $L = 2.5B(1 - \beta)$ (Achour et al., 2024). The calculated length L represents the optimal dimension, allowing the flow to naturally evolve towards a control section. This length is carefully selected to avoid being too long or too short, as both scenarios can negatively impact flow measurement accuracy.

The consequences of improper length selection include: If L is too long, pressure drop effects can no longer be neglected, rendering the theoretical assumptions invalid, and this may lead to inaccurate flow calculations due to energy losses within the device; If L is too short, the formation of a control section at the V-notch may be compromised, and there may be insufficient space for the flow to transition into a critical state properly. This will affect the device's proper functioning and prevent theoretical development.

The modified H-Flume ensures stable flow conditions and reliable discharge measurements by adhering to theoretical guidelines for length selection.

A key distinction between the original H-Flume and the modified version lies in their dimensional constraints. Original H-Flume features predefined standard dimensions, limiting its adaptability, while modified H-Flume does not have fixed dimensions. Its size is determined by the dimensions of the rectangular approach channel, particularly the width (B), and the depth (h_0).

This flexibility allows for customization based on site-specific requirements, making the modified H-Flume a versatile solution for diverse hydraulic applications.

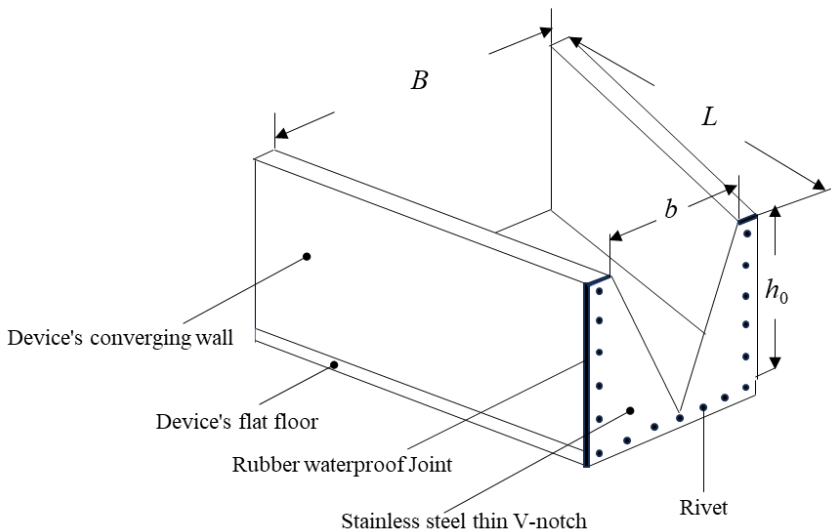


Figure 3: Perspective view of the modified H-Flume as tested in the laboratory

Dimensional analysis for the discharge Coefficient of the modified H-Flume

In this section, dimensional analysis is employed to develop the general form of the governing physical equation for the discharge coefficient of the modified H-Flume. This approach ensures that the resulting equation accurately describes the underlying physical phenomenon, is dimensionally correct, meaning that all terms are consistent with fundamental units, and accounts for influential variables in a reduced and simplified form.

As a first step, dimensional analysis requires identifying the influential variables affecting the discharge coefficient, and reducing the number of variables by transforming them into dimensionless parameters.

The selection of influential parameters in dimensional analysis is often based on engineering intuition and prior knowledge of fluid mechanics. In the present case, the following key variables influence the discharge (Q) of the modified H-Flume:

Q : Discharge (m^3/s) – the primary quantity of interest.

B : Approach channel width (m) – defines the inflow characteristics.

h_1 : Upstream flow depth (m) – determines the hydraulic head.

m : Side slope or apex angle of the V-notch, which affects flow contraction.

g : Acceleration due to gravity (m/s^2) – governs free-surface flow behavior.

ρ : Density of the fluid (kg/m^3) – influences flow properties.

μ : Dynamic viscosity of the fluid ($\text{Pa}\cdot\text{s}$) – accounts for fluid resistance.

σ : Surface tension (N/m) – relevant for small-scale flows.

The functional relationship linking these variables can be expressed as:

$$f(Q, \rho, g, B, h_1, \mu, \sigma, m) = 0 \quad (2)$$

This equation captures the interaction between the flow rate, geometric parameters, and fluid properties. To simplify this relationship, dimensional analysis techniques, such as the Buckingham π theorem will be applied (Langhaar, 1962), and the number of independent variables will be reduced into a set of dimensionless groups, making the equation more practical for theoretical and empirical modeling.

In the following sections, dimensional grouping techniques will be applied to further refine and express this functional relationship in a practical and computationally efficient form.

Following the identification of influential variables in the first step, the next essential step in dimensional analysis is the application of the Vaschy-Buckingham π theorem (Langhaar, 1962). This theorem is a fundamental tool used to transform a complex physical relationship into a more simplified, dimensionless form. By utilizing this theorem in combination with Equation (2), it is possible to derive a functional relationship

that expresses the discharge (Q) in terms of dimensionless parameters. This process allows the reduction of the number of independent variables, the derivation of a general equation that is universally applicable, and the identification of key dimensionless groups that govern the flow behavior.

By applying the Vaschy-Buckingham theorem, the final result obtained expresses the discharge (Q) as a function of a set of dimensionless parameters is as follows:

$$Q = \sqrt{g} m h_1^{5/2} \gamma \left(\frac{\rho \sqrt{g} h_1^{3/2}}{\mu}, \frac{\rho g h_1^2}{\sigma}, \frac{m h_1}{B} \right) \quad (3)$$

In hydraulic engineering, the stage-discharge relationship for a triangular weir is well-documented in the literature (Bos, 1989; Hager, 1986; Achour and Amara, 2021a). This standard form provides a theoretical foundation for analyzing flow behavior over a V-notch or a triangular outlet section.

By utilizing the established stage-discharge equation for triangular weirs and incorporating Eq. (3) from the present study, the following robust functional relationship for the discharge coefficient (C_d) can be derived as follows.

$$C_d = \gamma \left(\frac{\rho \sqrt{g} h_1^{3/2}}{\mu}, \frac{\rho g h_1^2}{\sigma}, \frac{m h_1}{B} \right) \quad (4)$$

This functional relationship allows for a generalized and scalable approach to predicting the discharge coefficient (C_d), a direct connection between theoretical models and empirical observations, ensuring accuracy in flow measurement applications, and improved controllability and reliability of the modified H-Flume, particularly in low and moderate flow conditions.

In the analysis of flow within the modified H-Flume, two fundamental dimensionless numbers naturally emerge from Eq. (4) namely, Reynolds number (Re) as the first term in brackets – Representing the ratio of inertial forces to viscous forces, and Weber number (We) as the second term in brackets – Representing the ratio of inertial forces to surface tension forces. These numbers provide insight into the dominant physical effects influencing the discharge behavior.

The effect of the Reynolds number (Re) is considered insignificant due to the turbulent flow regime present in the flume. In turbulent conditions, viscous forces are negligible compared to inertial forces, meaning that the discharge coefficient remains largely unaffected by viscosity. The effect of the Weber number (We) is also negligible because surface tension effects become relevant only at very low flow rates, where the upstream depth is extremely shallow, and small opening angles in the triangular cross-section could amplify surface tension effects, but such conditions are not present in the current experimental setup. Since the study is focused on moderate to high flow rates, where neither viscosity nor surface tension play a dominant role, these effects can be disregarded.

Given that Re and We do not significantly influence the flow behavior in this context, the governing equation (Eq. 5) can be simplified by eliminating these terms, leading to a more streamlined and practical relationship for discharge calculations. It reads as follows:

$$C_d = \varphi\left(\frac{mh_1}{B}\right) = \varphi(M_1) \quad (5)$$

Eq. (5) establishes that the discharge coefficient (C_d) of the modified H-Flume is solely dependent on the dimensionless parameter M_1 . This indicates that all other secondary effects, such as viscosity and surface tension, have been deemed insignificant, leaving M_1 as the primary governing factor.

The function φ , which defines the relationship between C_d and M_1 , will be rigorously derived in the next section based on established theoretical principles.

The parameter M_1 can be rewritten in a form that reveals its physical significance, as follows:

$$M_1 = \frac{\text{Triangular water area (depth } h_1, \text{ side slope } m)}{\text{Rectangular water area (width } B, \text{ same depth } h_1)}$$

This reformulation indicates that M_1 represents the section reduction factor, which quantifies the extent to which the flow cross-section is reduced due to the presence of the triangular outlet section in the modified H-Flume (Fig. 2).

The modified H-Flume is specifically designed such that $M_1 < 1$. This constraint ensures that the triangular section at the outlet effectively constrains the flow, leading to: 1) increased flow velocity due to flow contraction, 2) formation of a controlled critical flow section, which enhances measurement accuracy, and 3) optimized discharge coefficient behavior, making the device more predictable and reliable.

As will be revealed in the next section, the dimensionless parameter M_1 plays a crucial role in defining the discharge coefficient of the modified H-Flume. Acting in the capacity of a section reduction factor, it governs the flow transition through the device. The upcoming section will theoretically define the function φ , providing a detailed mathematical relationship for practical hydraulic applications.

THEORETICAL DERIVATION OF THE DISCHARGE COEFFICIENT RELATIONSHIP

The converging section of the modified H-Flume plays a crucial role in flow regulation by imposing a restriction on the flow, leading to: 1) Significant acceleration of the flow as it moves from a subcritical state upstream to a supercritical state downstream, 2) A decrease in flow depth due to the reduction in cross-sectional area, 3) An increase in velocity, governed by the principle of continuity and energy conservation. In addition,

this transformation, from a subcritical to a supercritical state, results in the formation of a control section at the V-notch outlet, which is essential for accurate flow measurement.

From a mathematical standpoint, the discharge (Q) is a single-valued function of the upstream depth (h_1). This implies that: 1) Each upstream depth within a given range uniquely corresponds to a specific discharge value, 2) The flow rate can be precisely determined by taking a single depth reading at a predefined measurement point, typically at the entrance cross-section of the device, 3) This principle forms the foundation of flume-based flow measurement, where the stage-discharge relationship (i.e., the function linking depth to discharge) is a fundamental concept.

The objective of this section is to theoretically derive the stage-discharge relationship for the modified H-Flume by first establishing the governing equation for the discharge coefficient (C_d). To achieve this goal, the authors propose two distinct theoretical approaches. The first method is based on the energy equation in dimensionless form. It utilizes the energy conservation principle, rewritten in dimensionless terms, to express the relationship governing C_d . The second method relies on the properties of a kinetic factor, which is closely linked to the approach flow velocity, providing an alternative means of deriving C_d . Interestingly, both methods yield identical results, reinforcing the theoretical validity of the derived discharge coefficient relationship.

As will be demonstrated, by employing these two theoretical approaches, the discharge coefficient (C_d) for the modified H-Flume can be rigorously established, leading to the derivation of the stage-discharge relationship.

Using the dimensionless energy equation

The critical depth in the rectangular cross-section 1-1 (Fig. 2) is written as:

$$h_{1c} = \left(\frac{Q^2}{gB^2} \right)^{1/3} \quad (6)$$

Let us remember that the subscript « c » denotes the critical conditions.

On the other hand, the critical flow depth in the V-notch weir in section 2-2 (Fig. 1 or Fig. 2) is as follows:

$$h_{2c} = \left(\frac{2Q^2}{gm^2} \right)^{1/5} \quad (7)$$

where $m = \cot \theta$

As it has been already specified in one of the previous sections, it is rightly assuming no pressure drop between sections 1-1 and 2-2 (Fig. 2). Equalling total heads between sections 1-1 and 2-2 translates into the following:

$$H_1 = H_2 = \frac{5}{4} h_{2,c} \quad (8)$$

The total head in the rectangular cross-section 1-1 (Fig. 2) can be written as:

$$H_1 = h_1 + \frac{Q^2}{2gB^2 h_1^2} \quad (9)$$

Taking into account Eqs. (8) and (9) yields what follows:

$$h_1 + \frac{Q^2}{2gB^2 h_1^2} = \frac{5}{4} h_{2,c} \quad (10)$$

Let us define the following relative upstream flow depth, capturing the hydraulic state of the upstream flow relative to critical conditions, as follows:

$$h_1^* = \frac{h_1}{h_{2,c}} \quad (11)$$

Dividing all members of Eq. (10) by $h_{2,c}$, and taking into account Eq. (11), results in what follows:

$$h_1^* + \frac{Q^2}{2gB^2 h_1^2 h_{2,c}} - \frac{5}{4} = 0 \quad (12)$$

Eliminating Q^2 between Eqs. (7) and (12) yields what follows:

$$h_1^* + \frac{h_{2,c}^5 g m^2}{4gB^2 h_1^2 h_{2,c}} - \frac{5}{4} = 0 \quad (13)$$

Multiplying and dividing the second member of Eq. (13) by h_1^2 , and simplifying, one may obtain the following:

$$h_1^* + \frac{h_{2,c}^4 m^2 h_1^2}{4B^2 h_1^4} - \frac{5}{4} = 0 \quad (14)$$

Eq. (14) reduces to what follows:

$$h_1^* + \frac{M_1^2}{4h_1^{*4}} - \frac{5}{4} = 0 \quad (15)$$

Eq. (15) can be put in the following final form:

$$h_1^{*5} - \frac{5}{4} h_1^{*4} + \frac{1}{4} M_1^2 = 0 \quad (16)$$

In practical applications, the user typically has knowledge of the dimensionless parameter M_1 , since the parameters m (side slope), h_1 (upstream depth), and B (approach channel width) are given. Thus, Eq. (16) serves as a tool to compute the relative upstream depth h_1^* . However, this equation is not explicit, meaning that approximations are required for its resolution. The following methods may be used to determine h_1^* : 1) Graphical interpretation allowing extracting h_1^* values from a plotted curve, 2) Trial-and-Error method using iterative substitution until convergence, 3) Numerical computation using a calculation program or root-finding algorithms for precise values.

Since the flow in section 1-1 (Fig. 2) is in a subcritical regime, the upstream depth h_1 is strictly greater than the critical depth $h_{2,c}$ in the V-notch, meaning that $h_1^* > 1$ according to Eq. (11). For values of h_1^* having physical meaning, and according to the exact Eq. (16), the behavior of h_1^* as a function of M_1 is depicted in Fig. 4, where: 1) h_1^* decreases as M_1 increases, indicating that a higher section reduction factor (M_1) leads to a shallower relative upstream depth, 2) The relationship satisfies the following particular and extreme conditions $(M_1; h_1^*) = (0; 0.125)$ and $(M_1; h_1^*) = (1; 1)$.

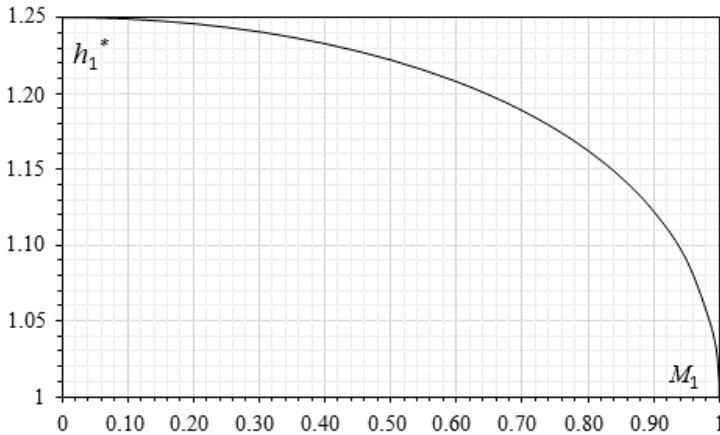


Figure 4: Variation in $h_1^*(M_1)$ according to Eq. (16)

The dimensionless parameter M_1 , previously mathematically defined, quantifies the degree of flow contraction due to the V-notch configuration in the modified H-Flume.

The extreme cases $M_1 \rightarrow 0$ and $M_1 \rightarrow 1$ could be examined purely from a theoretical perspective. However, their actual occurrence in the modified H-Flume depends on practical design constraints and real-world flow conditions.

In practical reality, the modified H-Flume is designed specifically to create a flow contraction, so complete absence of contraction, i.e., $M_1 = 0$, is not physically possible. It is theoretical expected that the V-notch effect vanishes, and the flow behaves as if it were in an ordinary rectangular channel. Even in very wide channels, some degree of contraction will always exist due to the presence of the V-notch outlet. In addition, if M_1 were to approach 0, the flume would lose its ability to control the flow rate, negating its

intended purpose. The other extreme case $M_1 \rightarrow 1$ is theoretically possible but rare. This scenario would require the entire flow to pass through only the V-notch, meaning that the flow is entirely confined within the V-notch. In this case, the rectangular approach section does not contribute to the discharge. This would mean an extremely narrow approach channel or a very large notch relative to the channel width. While this is theoretically possible, it is not a typical operating condition, as flumes are generally designed to maintain some rectangular section contribution to flow for stability. Full contraction could lead to excessive velocity and flow instability, making the modified H-Flume an impractical design choice.

In real-world applications, M_1 typically ranges from 0.05 to 0.95, ensuring, a controlled contraction for accurate discharge measurement, a flow stability while maintaining a well-defined control section, an avoidance of extreme flow sensitivity, which could lead to unpredictable variations in measurements.

A detailed study of the variation of $h_1^*(M_1)$, as depicted in Fig. 4, reveals that the curve follows the shape of a quarter of an ellipse. This geometric insight is valuable as it allows for: 1) A more accurate approximation of the implicit function described by Eq. (16), 2) The derivation of an explicit approximate formula to replace the implicit form, thereby simplifying computational efforts. Thus, by leveraging the mathematical properties of an ellipse, the authors recommend the following explicit $h_1^*(M_1)$ relationship:

$$h_1^* = 0.253(1 - M_1^2)^{0.428} + 0.998 \quad (17)$$

The approximate Eq. (17) is a practical and efficient tool for calculating $h_1^*(M_1)$, within the following broad validity range $0.05 \leq M_1 \leq 0.95$. This range covers all practical cases encountered in flow measurement applications, making it a highly useful approximation. In addition, Eq. (17) is remarkably accurate, introducing only a maximum deviation of 0.094% when computing the relative upstream flow depth h_1^* . For more demanding practitioners who require higher precision, the authors have developed in appendix an even more accurate explicit relationship for $h_1^*(M_1)$. This new formulation offers a maximum deviation of only 0.00185% in the computation of h_1^* , a corresponding deviation of just 0.00463% in the calculation of the modified H-Flume discharge coefficient. Furthermore, unlike Eq. (17), which is limited to a specific range, this new explicit equation is valid for the entire range of M_1 , i.e., $0 \leq M_1 \leq 1$. However, despite its superior accuracy, the newly derived explicit equation has certain drawbacks as it is mathematically cumbersome and less convenient to use in routine calculations. Given this trade-off, users can select between Eq. (17) for general-purpose applications, where a deviation of 0.094% is acceptable, or the new explicit relationship for high-precision scenarios, where minimal deviation is required.

Eq. (17) is recommended for most engineering applications due to its simplicity and high accuracy within the practical range, while the more complex explicit equation, developed in appendix, is suitable for advanced studies and highly sensitive measurements, where even minimal errors must be avoided.

To establish the stage-discharge relationship for the modified H-Flume, a key step involves eliminating the critical depth ($h_{2,c}$) from Eqs. (7) and (11). This mathematical operation leads to a generalized stage-discharge formula, which directly relates the discharge (Q) to the upstream depth (h_1). It reads as follows:

$$Q = \frac{1}{2} \sqrt{2g} m h_1^{*-5/2} h_1^{5/2} \quad (18)$$

The resulting Eq. (18) follows the standard stage-discharge formulation, where the flow rate (Q) is a single-valued function of the upstream depth h_1 . This ensures that each measured upstream depth uniquely determines the discharge, making flow measurement straightforward and reliable.

In addition, this theoretically refined approach enhances the accuracy and usability of the modified H-Flume as a flow measurement device.

When determining the side slope (m) of the V-notch in the modified H-Flume, it is not advisable to directly measure the angle θ (Fig. 1). The reason for this recommendation is that angle measurements (θ -slope) are prone to systematic reading errors due to instrument limitations and human inaccuracies. In addition, small measurement deviations in θ can lead to significant errors in the calculated side slope, affecting the accuracy of flow measurement computations. Since the top width (b) and the depth (h_0) of the device can be easily and precisely measured, it is recommended to compute the side slope (m) using the following relationship:

$$m = \frac{b}{2h_0} \quad (19)$$

This formula ensures greater accuracy by relying on directly measurable dimensions rather than an angle-based calculation, reduction of potential errors, enhancing the reliability of flow computations, and better practical application, as measuring b and h_0 is straightforward using standard tools such as calipers or rulers.

The stage-discharge relationship governing triangular cross-sections, such as triangular weirs, follows a well-established formula. This standard form has been widely recognized in the literature (Bos, 1989; Hager, 1986; Achour and Amara, 2021a; 2021b; 2022; 2023; Achour and De Lapray, 2023). This relationship is particularly applicable to the V-notch of the modified H-Flume, which functions similarly to a suppressed triangular weir without a crest height. Since the modified H-Flume's discharge is governed by a triangular cross-section at the outlet, the same stage-discharge equation applies. This means: the flow rate through the V-notch behaves similarly to that of a triangular weir, the discharge is directly related to the upstream depth (h_1), and the flow characteristics remain consistent with standard triangular weir hydraulics.

In addition, the equation is valid as long as free flow conditions exist at the notch, meaning the flow is not submerged downstream. The governing equation can be expressed as follows:

$$Q = \frac{8}{15} C_d m \sqrt{2g} h_1^{5/2} \quad (20)$$

As hydraulic applications: The V-notch in the modified H-Flume creates a critical flow condition, ensuring a well-defined control section for accurate flow measurement. The flow rate sensitivity to depth follows a power-law relationship, meaning small changes in upstream depth lead to significant changes in discharge. The absence of a crest height simplifies the derivation of the equation and makes it more applicable to open-channel conditions.

By comparing Eqs. (18) and (20), one may obtain the following exact discharge coefficient C_d relationship for the modified H-Flume:

$$C_d = \frac{15}{16} h_1^{*-5/2} \quad (21)$$

This relationship is significant because it depends solely on the upstream relative flow depth h_1^* , and it is consequently linked to the section reduction parameter M_1 as defined by Eq. (16). This means that the discharge coefficient can be expressed as a function of M_1 , allowing for a direct evaluation of C_d without requiring additional experimental calibration.

Since C_d is fully determined by upstream conditions, the discharge equation becomes more predictable and accurate for flow measurement applications. Unlike conventional empirical formulations, this derived relationship ensures that C_d is based on theoretical derivations rather than experimental adjustments. This relationship simplifies the stage-discharge equation of the modified H-Flume and provides a direct link between geometry and discharge coefficient.

Hydraulic engineers can now compute C_d directly from upstream parameters without the need for complex calibration. The derived expression ensures that:

$$C_d = f(h_1^*) = f(M_1) \quad (22)$$

Since C_d depends on M_1 , thus m , and h_1/B are C_d 's only influential non-dimensional parameters. As shown in one of the previous sections, dimensional analysis predicted this result. This confirms that dimensional analysis correctly identifies C_d 's dependency on M_1 and the associated non-dimensional parameters.

Fig. 5 illustrates how C_d varies with M_1 based on Eq. (16) and Eq. (21).

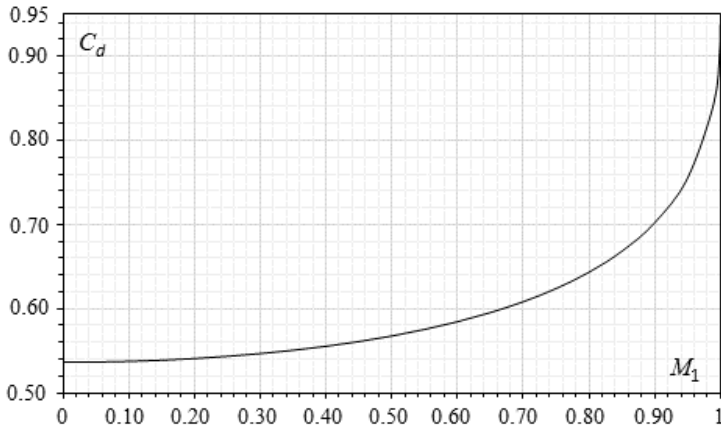


Figure 5: Variation in the modified H-Flume discharge coefficient C_d as a function of M_1 , according to Eq. (16) along with Eq. (21)

Fig. 5 reveals that as M_1 increases, the flow contraction effect weakens, leading to a gradual increase in C_d . Moreover, C_d increases rapidly in the range of high values of M_1 , reaching the value 0.9375 as M_1 tends asymptotically towards 1.

The readers should be reminded that the primary objective of the study is not to design a device that maximizes discharge capacity by increasing the discharge coefficient C_d . Instead, the study focuses on developing a device that ensures precise estimation of the conveyed flow rate in a given rectangular approach channel. Fig. 5 presents high values of C_d , but these should not be misinterpreted as the primary concern of the study. High C_d values are not relevant to the research objectives and will not be analyzed further. Maximizing C_d differs from optimizing flow measurement.

By inserting Eq. (17) into Eq. (21), the study derives an approximate governing relationship for the discharge coefficient C_d in the modified H-Flume. This equation provides a simplified yet accurate expression for predicting C_d based on fundamental flow parameters.

$$C_{d,appr} = \frac{15}{16} \left[0.253(1 - M_1^2)^{0.428} + 0.998 \right]^{-5/2} \quad (23)$$

where the subscript “*appr*” denotes “Approximate”.

The study establishes that within the validity range $0.05 \leq M_1 \leq 0.95$, the approximate Eq. (23) introduces a maximal deviation of only 0.235% in computing the modified H-Flume discharge coefficient C_d . This maximal deviation confirms the robustness and reliability of the approximate equation as a practical alternative to exact formulations.

The study anticipates this deviation based on Eq. (21), since one may write the following:

$$\left(\frac{\Delta C_d}{C_d}\right)_{\max} = \frac{5}{2} \left(\frac{\Delta h_1^*}{h_1^*}\right)_{\max} = \frac{5}{2} \times 0.094 = 0.235\% \quad (24)$$

This predictability reinforces the theoretical consistency of the approximation. The new approximate C_d formulation integrates key flow characteristics, ensuring better accuracy and ease of use. The derived equation reduces computational complexity, making C_d estimation more straightforward. This confirmation eliminates concerns about approximation errors, ensuring that Eq. (23) can be applied with high confidence. If Eq. (23) aligns with measured values, it will confirm that the modified H-Flume operates within predictable limits. The approximation should be evaluated under different flow conditions to ensure its validity.

One could provides the following insights into the impact of using the approximate Eq. (23) on the discharge coefficient C_d . Specifically, Fig. 6 illustrates the percentage deviations that arise when using this approximation within the validity range $0.05 \leq M_1 \leq 0.95$, which ensures that extreme cases of contraction, i.e., very small or very large M_1 , are not considered in this analysis.

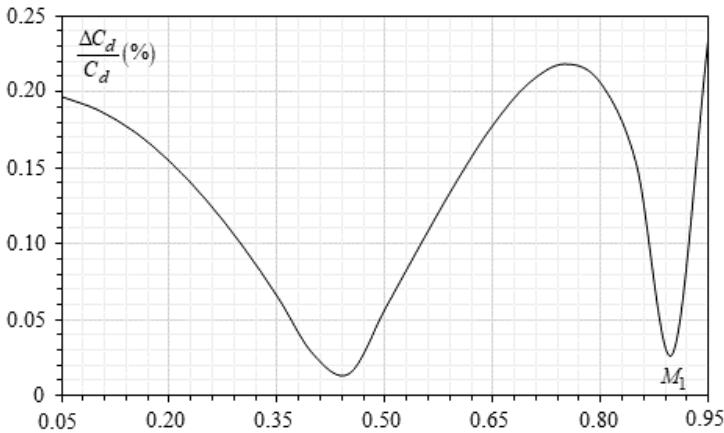


Figure 6: Percentage distribution of deviations induced by the approximate Eq. (23) in the computation of the discharge coefficient C_d , within the validity range $0.05 \leq M_1 \leq 0.95$

Fig. 6 indicates, in particular, that the maximum deviation of 0.235%, caused by the approximate Eq. (23) in the discharge coefficient C_d calculation, is obtained for the largest value of the dimensionless parameter M_1 , i.e. $M_1 = 0.95$. This maximum deviation is extremely low, confirming the reliability of Eq. (23). Restricting M_1 to $0.05 \leq M_1 \leq 0.90$ further reduces the deviation to 0.218%, improving accuracy. These findings indicate that hydraulic structures designed with the approximate Eq. (23) will operate within expected

accuracy levels. Engineers can use Eq. (23) without concerns about significant errors in discharge estimations.

Using the kinetic factor

Eq. (10) can be rewritten as follows:

$$h_1 \left(1 + \frac{Q^2}{2gB^2h_1^3} \right) = \frac{5}{4} h_{2,c} \tag{25}$$

Eliminating Q^2 between Eqs. (25) and (7) yields the following:

$$h_1 \left(1 + \frac{gm^2h_{2,c}^5}{4gB^2h_1^3} \right) = \frac{5}{4} h_{2,c} \tag{26}$$

Multiplying and dividing by h_1^2 the second member of Eq. (26), which is in parentheses, results in what follows:

$$h_1 \left(1 + \frac{m^2h_{2,c}^5h_1^2}{4B^2h_1^5} \right) = \frac{5}{4} h_{2,c} \tag{27}$$

Eq. (27) can be rewritten in the following form:

$$h_1 \left[1 + \frac{(mh_1/B)^2}{4(h_1/h_{2,c})^5} \right] = \frac{5}{4} h_{2,c} \tag{28}$$

One may therefore rightly write Eq. (28) in the following simplified form:

$$h_1 \left(1 + \frac{M_1^2}{4h_1^{*5}} \right) = \frac{5}{4} h_{2,c} \tag{29}$$

Let us rewrite Eq. (29) as follows:

$$h_1(1 + \delta) = \frac{5}{4} h_{2,c} \tag{29a}$$

where δ is the kinetic factor, closely related to the approach flow velocity; it is written as follows:

$$\delta = \frac{M_1^2}{4h_1^{*5}} \tag{30}$$

The kinetic factor δ is fundamental in hydraulic computations, as it accounts for velocity effects in flow analysis, ensuring more accurate hydraulic computations. It is easy to provide a direct mathematical relationship between δ and the mean approach flow velocity; it reads as $\delta = V_1^2 / (2gh_1)$. Moreover, δ can be written as $\delta = \left(V_1 / \sqrt{2gh_1} \right)^2$, which physically means that the kinetic factor δ represents the square of the velocity ratio between the actual flow and the ideal theoretical velocity from Torricelli's law, where h_1 is considered to be the vertical height between the free level of the water and the V-notch opening through which the liquid flows.

Considering Eq. (16), Eq. (30) shows that the kinetic factor δ is controlled exclusively by the dimensionless section reduction parameter M_1 . This implies that all variations in δ are a direct result of changes in M_1 . This finding is significant for understanding flow velocity effects in hydraulic systems. In addition, calculations reveal that the kinetic factor δ is less than 1, while varying within the range $0 \leq \delta \leq 0.25$ as M_1 varies within the range $0 \leq M_1 \leq 1$. The kinetic factor δ increases as M_1 increases, and this trend is illustrated in Fig. 7.

Inserting Eq. (7) into Eq. (29a) yields the following:

$$\left(\frac{2Q^2}{gm^2} \right)^{1/5} = \frac{4}{5} (1 + \delta) h_1 \quad (31)$$

This allows us to write the discharge Q in the following form:

$$Q = \frac{1}{2} \left(\frac{4}{5} \right)^{5/2} m \sqrt{2g} (1 + \delta)^{5/2} h_1^{5/2} \quad (32)$$

Furthermore, comparing Eq. (32) with Eq. (20) yields the following discharge coefficient C_d relationship:

$$C_d = C_0 (1 + \delta)^{5/2} \quad (33)$$

where C_0 is a constant defined as follows:

$$C_0 = \frac{15}{16} \left(\frac{4}{5} \right)^{5/2} \quad (34)$$

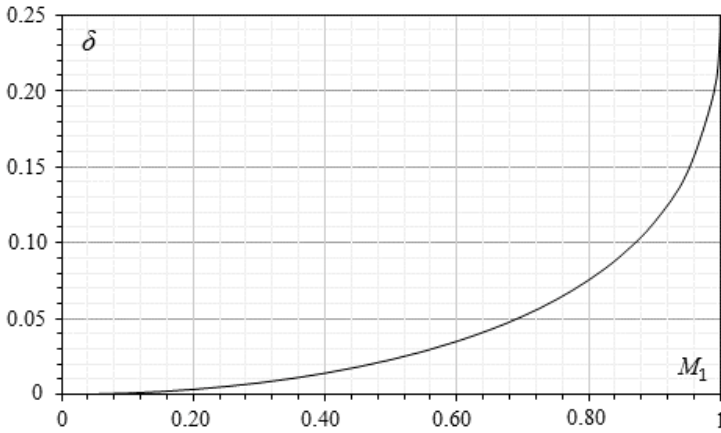


Figure 7: Variation in $\delta(M_1)$ according to Eq. (30) along with Eq. (16)

According to Eqs. (30) and (33), one may write the C_d discharge coefficient relationship in the following final form:

$$C_d = C_0 \left(1 + \frac{M_1^2}{4h_1^{*5}} \right)^{5/2} \tag{35}$$

where the relative upstream depth h_1^* can be accurately calculated using the approximate Eq. (17). This confirms that C_d inherently includes kinetic energy effects, making the modified H-Flume’s discharge estimation more precise. Integrating the kinetic factor δ , ensures that velocity energy effects are naturally incorporated into the discharge formulation.

Eq. (35) represents the second formulation of the modified H-Flume discharge coefficient C_d , derived by incorporating the properties of the kinetic factor δ . This equation provides additional confirmation that C_d is solely governed by the dimensionless section reduction parameter M_1 . Since M_1 is composed of the slope ratio m and the relative depth h_1/B , the discharge coefficient indirectly depends on these variables. This formulation reinforces the theoretical soundness of using M_1 as the primary governing variable for flow contraction effects.

Although they are derived from two different methods, Eqs. (21) and (35) give stringently the same result.

Although the kinetic factor δ is always less than 1, it should not be neglected in discharge computations. Many flow measurement studies unfairly omit the effect of δ , leading to fatal errors in discharge coefficient calculations. Neglecting δ removes the effect of approach flow velocity, assuming that kinetic energy contributions are negligible. The governing Eq. (35) for C_d contains the term $(1+\delta)$, which is not necessarily close to 1. Omitting δ means treating $(1+\delta)$ as exactly 1, leading to inaccurate discharge estimates.

If δ is ignored, the predicted discharge will be lower than the actual value, causing measurement discrepancies.

To highlight the consequences of omitting the δ kinetic factor, let us take the following practical value $M_1 = 0.40$. For this case, Eq. (30), along with Eq. (16), gives $\delta = 0.01405454$, i.e., $(1+\delta)^{5/2} = 1.03550757$. According to Eqs. (33) and (34), the exact discharge coefficient value is $C_d = 0.55571168$. When neglecting the effect of the kinetic factor δ , i.e., setting $\delta = 0$, Eqs. (33) and (34) give $C_{d,appr} = C_0 = 0.53665631$. Thus, neglecting the effect of the approach flow velocity, which amounts to ignoring the impact of δ , leads to a deviation of more than 3.4% in the C_d discharge coefficient estimation. A 3.4% error in C_d leads to an equivalent error in flow rate estimation, which is problematic in precision hydraulic applications.

Flow measurement devices such as H-Flumes and V-notch weirs require highly accurate discharge coefficients. Ignoring δ results in systematic underestimation of discharge rates, making flow control and regulation less reliable.

EXPERIMENTAL VALIDATION

The experimental validation phase of the study is crucial for testing and refining the theoretical relationships previously developed. The main objective is to evaluate the accuracy of the approximate explicit Eq. (23), which governs the discharge coefficient C_d of the modified H-Flume. The experiments test whether the theoretical predictions of C_d align with real-world measurements. If deviations exist between the predicted and measured C_d values, adjustments will be made to the constants in Eq. (23) to improve its accuracy. Recall that that C_d is exclusively influenced by the dimensionless section reduction parameter M_1 , which consists of the side slope m of the V-notch, i.e., m horizontal to 1 vertical, the upstream depth h_1 , the width B of the approach channel or device inlet, as depicted in the hydraulic test platform of Fig. 8.

The validation process is carried out on four modified H-Flumes. The experimental study ensures that flow conditions, measurement techniques, and data processing meet high experimental standards.

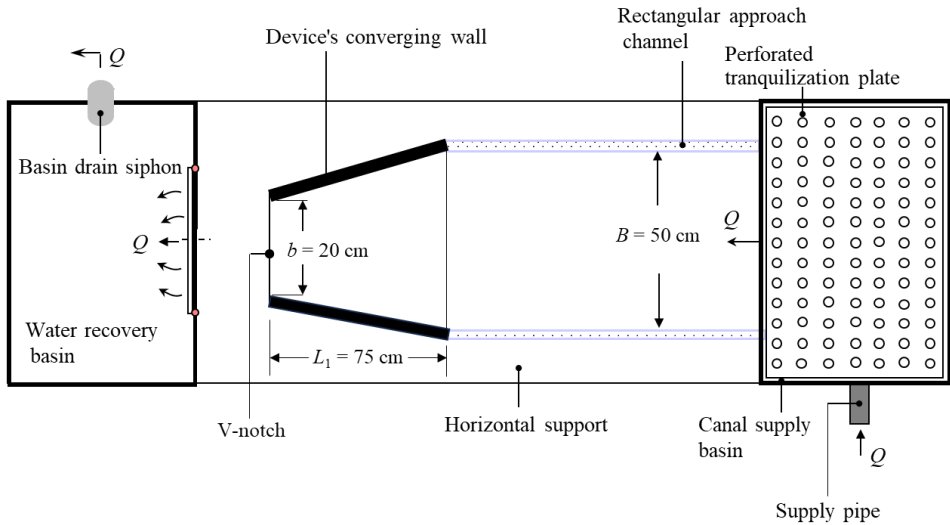


Figure 8: A prototype of the modified H-Flume undergoing experimental evaluation on a custom-designed hydraulic platform (dimensions presented are not to scale)

The experimental discharge coefficient $C_{d,exp}$ is derived from Eq. (20), providing a practical method for determining C_d based on measured discharge values. This formulation is crucial for validating the theoretical model and ensuring consistency between computed and observed results. The experimental discharge coefficient is obtained using measured data from the hydraulic test setup. It allows for direct comparison with the theoretical predictions given by Eq. (23). The derived $C_{d,exp}$ relationship is as follows:

$$C_{d,Exp} = \frac{15}{8} \frac{Q_{Exp}}{m \sqrt{2g} h_{1,Exp}^{5/2}} \quad (36)$$

where the subscript “Exp” denotes “Experimental”, while the subscript “Th” will be used later to refer to “Theoretical”.

The experimental validation of the modified H-Flume relies on precise measurements of the discharge Q and the upstream flow depth h_1 . Since these parameters directly affect the computation of the discharge coefficient C_d , their accuracy is of utmost importance.

The experimental discharge Q was not measured directly but computed as the average of the ultrasonic flow meter reading and the magnetic flow meter reading. Both measurement devices were carefully calibrated to minimize errors. The absolute error in this procedure was 0.1 L/s, ensuring high precision in flow rate estimation. Since Q_{Exp} directly influences $C_{d,Exp}$, reducing systematic errors in flow rate measurement improves the reliability of the study’s conclusions. The upstream flow depth $h_{1,Exp}$ was measured

using a double-precision Vernier point gauge, which was graduated to 1/10th of a millimeter. The absolute error in $h_{1,Exp}$ measurements was 0.02 mm. The shallowest depth measured was 100 mm, giving a maximum relative deviation of only $100 \times 0.02/100 = 0.02\%$. Small errors in reading $h_{1,Exp}$ lead to large uncertainties in $C_{d,Exp}$, so maintaining a 0.02% precision level ensures accurate results. The use of a high-precision Vernier gauge confirms the commitment to minimizing experimental uncertainty. This methodological rigor enhances the reliability of the experimental validation of the modified H-Flume discharge equation. The parameter m was not measured but calculated with great precision by Eq. (19) since the top width b of the V-notch and the device's depth h_0 are given for the designed installation.

The experimental discharge Q_{Exp} and the upstream flow depth $h_{1,Exp}$ were varied over a wide practical range, ensuring that the modified H-Flume was tested under different flow conditions. The discharge was tested across the following broad range $1.136 \text{ L/s} \leq Q_{Exp} \leq 69.71 \text{ L/s}$. This ensures that the experimental model covers both low-flow and high-flow conditions, making the results applicable to real-world hydraulic scenarios. The wide range of Q_{Exp} allows evaluation of flow contraction effects at different discharges. The tested range of experimental flow rates resulted in upstream depth h_1 varying in the following range $10 \text{ cm} \leq h_1 \leq 47.8 \text{ cm}$. Testing across small and large depths helps validate whether the theoretical equation holds across varying approach flow conditions.

Four modified H-Flumes of the same depth h_0 were tested, with details provided in Table 1. The converging walls and approach channel walls were constructed using 2.5 cm thick plexiglass plates. The flat floors of the device and approach channel were 1.5 cm thick, also made of plexiglass for sufficient structural rigidity.

To ensure leak-proof assembly, the walls, including those of the approach channel and the device, were bonded to the floor using chloroform injection, a technique known for its high polymerization efficiency in plexiglass. This operation guarantees excellent sealing, preventing leaks that could alter the experimental discharge measurements, and ensures long-term durability and mechanical stability of the testing setup.

The tests included different rectangular approach channel widths B as listed in Table 1. Changing B allowed the study to explore different contraction rates β , width ratio between throat and approach sections. This variability is essential for assessing the effect of approach channel geometry on flow contraction and C_d values.

Table 1: Geometric properties of the four modified H-Flumes subjected to laboratory testing

Device	m	h_0 (cm)	B (cm)	b (cm)	β	L_1 (cm)
1	0.18	50	40	18	0.45	55
2	0.20	50	50	20	0.40	75
3	0.28	50	60	28.2	0.47	79.5
4	0.35	50	70	35	0.50	87.5

On the other hand, Table 2 provides a detailed breakdown of the experimental values, offering insights into the influence of approach flow parameters on discharge characteristics.

The adopted hydraulic conditions for the four modified H-Flumes validation allowed collecting nearly 1540 data points corresponding to experimental discharge Q_{Exp} and upstream depth $h_{1,Exp}$. The details of these values, organized by device, are reported in Table 2. Collecting 1540 measured data points ensure that the validation of Eq. (23) governing C_d is statistically robust. The large sample size allows for detailed error analysis and refinement of theoretical predictions. The experimental values of M_1 confirm that they fall within the validity range of the approximate theoretical Eq. (23). This ensures that the theoretical discharge coefficient model remains applicable to real-world conditions.

Table 2: Hydraulic parameters observed throughout the laboratory testing procedure

Device	Number of measures	Range of $h_{1,Exp}$ (cm)	Range of Q_{Exp} (l/s)	Range of M_1 (Exp.)
1	385	[12; 47.8]	[1.136; 36.33]	[0.054; 0.2151]
2	360	[12.5; 47.03]	[1.398; 38.66]	[0.05; 0.1881]
3	366	[10.8; 47.02]	[1.358; 54.28]	[0.0504; 0.2194]
4	427	[10; 47.5]	[1.40; 69.71]	[0.05; 0.2375]

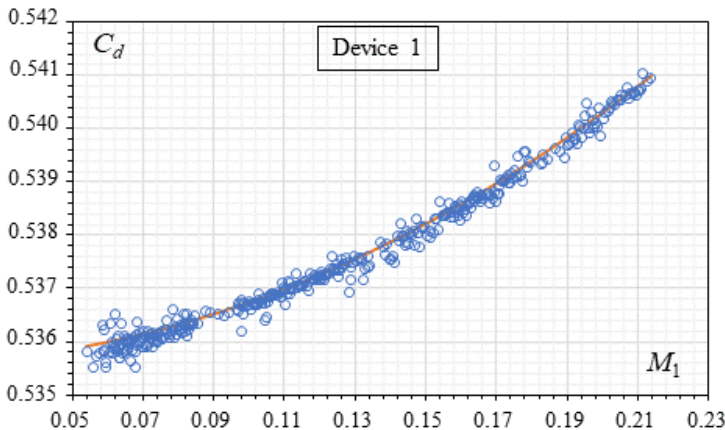
The dataset includes measurements across different flow conditions, enhancing the generality of the derived discharge equation. By covering a wide range of flow conditions, the dataset provides a strong empirical basis for validating and refining the theoretical model for C_d , if discrepancies between theoretical and experimental C_d values exist.

The theoretical discharge coefficient C_d , computed using the approximate Eq. (23), was compared with experimental observations for the four tested devices. The results, illustrated in Fig. 9, confirm the high accuracy of the theoretical model. The vast majority of experimental data points align well with the theoretical curve in orange, based on Eq. (23). For devices 3 and 4, the experimental data is so closely clustered around the theoretical curve that obscured it, meaning a near-perfect agreement between predicted and observed C_d values, demonstrating the robustness of the theoretical model in different flume configurations.

A few data points slightly deviate from the theoretical trend. These deviations are likely due to minor experimental errors, such as reading errors in upstream depth $h_{1,Exp}$, inaccuracies in measured discharge Q_{Exp} , or possible combined measurement uncertainties. In no way do these few outlying points of the curve call into question the validity of the approximate theoretical Eq. (23).

Since the vast majority of experimental observations follow the theoretical curve, Eq. (23) is confirmed to be highly reliable. No empirical corrections are required, proving that the model accurately predicts the discharge coefficient for the modified H-Flume.

It is worth noting, that the tests conducted on the four modified H-Flumes confirmed that the strict verticality of the V-notch did not introduce any significant hydraulic constraints. This is an important finding, as it addresses common concerns related to flow behavior in such configurations. There was observed no excessive flow acceleration which is one potential issue with a strictly vertical V-notch; this could have made it difficult to maintain critical depth, or could have altering flow profiles, leading to inconsistent discharge coefficients. The experimental results showed that this was not the case, meaning the design effectively controls velocity. In addition, no increased turbulence which could have leading to measurement errors was observed; it is well-known that, in some cases, vertical V-notches can cause significant turbulence, which disrupts free-flow conditions, or introduces instabilities in depth readings, affecting discharge computation accuracy. The tests confirmed that turbulence remained within acceptable limits, ensuring precise flow measurements. Moreover, no flow control issues due to rapid water passage was observed during tests, knowing that a major concern with vertical V-notches is that: water might pass through too quickly, and reducing the ability to control and regulate flow, compromise the hydraulic stability of the measuring section. The tests showed that the flow remained well-regulated, meaning that the notch design allows for effective discharge measurement. This finding supports the use of vertical V-notches in real-world applications, such as: irrigation system flow monitoring, hydraulic lab experiments for discharge calibration, and flood monitoring structures where precise flow control is needed. All these considerations validate the modified H-Flume-based vertical V-notch design as a reliable approach for accurate flow measurement and discharge computation.



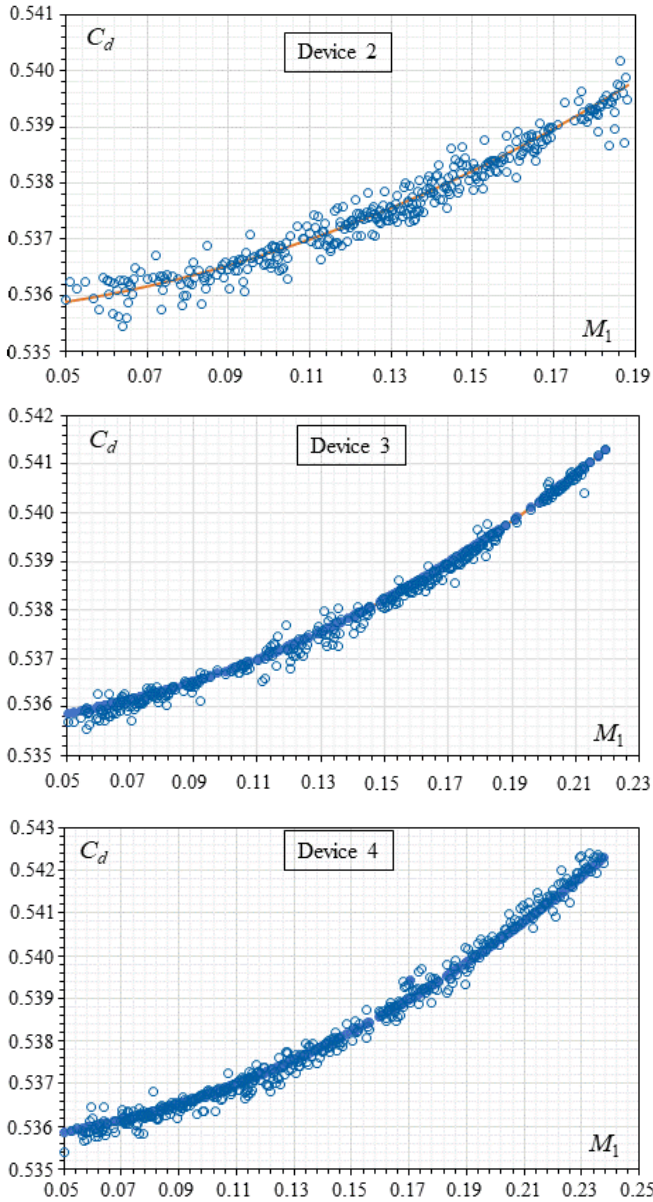


Figure 9: Variation in $C_d(M_1)$ for the four tested devices outlined in Table 1. The orange line represents the predicted C_d derived from Eq. (23), while open markers denote the experimentally observed C_d computed using Eq. (36)

To provide a clear assessment of the reliability of Eq. (23), the authors present Table 3, which summarizes the maximum deviation between theoretical and experimental discharge coefficients C_d . The results confirm that the approximate Eq. (23) is highly reliable, as its deviations remain well within acceptable limits across all four tested devices. The largest deviation observed, i.e., 0.185%, remains below acceptable engineering tolerance levels, even significantly smaller than what is typically required for flow measurement accuracy in hydraulic structures. This confirms once again that Eq. (23) does not require empirical corrections, making it robust for real-world applications. In other words, this means that Eq. (23) outperforms expectations, further validating its theoretical foundation.

Table 3: Deviation in the C_d computation resulting from the application of the approximate Eq. (23)

Device	Deviation $\Delta C_d / C_d$ (%)		
	Minimum	Maximum	Average
1	2.765E-05	0.115	0.0231
2	2.2E-04	0.185	0.0315
3	1.591E-05	0.0957	0.0211
4	2.454E-05	0.0979	0.0257

CONCLUSION

Accurate flow measurement in open channels and pipes has long been a critical challenge in hydraulics. Numerous gauging methods have been developed to address this issue, with the most well-known being free-spilling flow devices such as weirs and flumes. Among these, weirs—characterized by their sharp crests or notches (V-shaped, rectangular, parabolic, etc.)—are particularly popular due to their precision in flow measurement. For instance, V-notch weirs, also known as Thomson weirs, offer superior accuracy for low and high flow rates. However, weirs with a rectangular notch can become less precise for very low flow rates or when lateral contraction effects are present.

Flumes, another widely used category of flow measurement devices, overcome some of the limitations of weirs. They are designed to regulate and measure flow rates by channeling water through specifically shaped sections. Among the many types of flumes, the H-Flume, developed in the mid-20th century, is notable for its simplicity and versatility in measuring low to moderate flows. The original H-Flume features a trapezoidal terminal section with beveled vertical walls, which approximates a V-notch shape but lacks the geometrical rigor for theoretical analysis. As a result, its discharge coefficient and stage-discharge relationships have traditionally been derived from empirical data, leading to inaccuracies and limitations in precision.

The need for improvement in H-Flume design has motivated the current study. The modified H-Flume presented here introduces a vertical V-notch at the terminal section, which enhances its geometric consistency and allows for rigorous theoretical derivation

of the discharge coefficient (C_d) and flow rate (Q). This configuration combines the advantages of the V-notch's precision with the practicality of the H-Flume structure, resulting in a device that is more accurate, reliable, and adaptable to various hydraulic conditions.

In this study, the modified H-Flume is examined both theoretically and experimentally. Dimensional analysis and energy principles are employed to derive explicit and implicit relationships governing the discharge coefficient and the stage-discharge relationship. Laboratory testing of four modified H-Flumes with varying geometries validates the theoretical models and demonstrates the device's accuracy across a wide range of flow conditions. As a result, the theoretical relationships governing the discharge coefficient and, hence, the flow rate require no correction or adjustment.

The findings establish the modified H-Flume as a significant advancement in open-channel flow measurement, capable of overcoming the limitations of its predecessors while maintaining simplicity and reliability.

As a conclusion of results, the modified H-Flume significantly improves the accuracy and reliability of flow measurement in rectangular channels. It combines theoretical rigor with practical utility, providing precise discharge predictions with minimal deviation, thus advancing the state of open-channel hydraulics.

The modified H-Flume is based on a strictly triangular vertical terminal section, which differs from the traditional trapezoidal terminal section. This modification addresses several drawbacks observed in conventional designs, making it a potentially wise choice for flow measurement applications.

MAIN RESULTS

The study of the modified H-Flume yielded several key findings as follows:

Justification for Adopting the Modified H-Flume

The modified H-Flume is based on a strictly triangular vertical terminal section, which differs from the traditional trapezoidal terminal section. This modification addresses several drawbacks observed in conventional designs, making it a potentially wise choice for flow measurement applications.

Key Advantages of the Modified H-Flume

Elimination of Unwanted Hydraulic Effects

Experimental observations indicate that the drawbacks of traditional H-Flumes (e.g., turbulence, energy losses, and inconsistent discharge coefficients) are not present in the modified version. This suggests that the strictly triangular terminal section leads to smoother, more predictable flow conditions.

Improved Flow Measurement Accuracy

The triangular vertical section ensures a well-defined control section, allowing for: Stable critical depth formation; Reduced uncertainties in discharge calculations; Unlike the trapezoidal outlet, which may cause variations in flow contraction, the triangular design maintains a uniform contraction effect.

Simplified Theoretical Modeling

The modified design aligns well with standard triangular weir equations, reducing the need for complex empirical corrections. This makes calibrations easier and improves predictive accuracy.

Enhanced Structural Stability and Fabrication Simplicity

The strictly triangular terminal section may allow for simpler construction and lower material use compared to a trapezoidal outlet with a small base. This contributes to cost efficiency while maintaining high performance.

Theoretical Relationships

The discharge coefficient (C_d) and stage-discharge relationships for the modified H-Flume were derived using rigorous theoretical methods, including dimensional analysis and energy principles.

An implicit relationship between the section reduction factor ($M_1 = mh_1/B$) and the upstream relative flow depth ($h_1^* = h_1/h_{2,c}$) was established.

An explicit approximate equation for $h_1^*(M_1)$ was proposed to simplify calculations, achieving a maximum deviation of only 0.094% compared to the exact implicit relationship.

Experimental Validation

Laboratory testing of four modified H-Flumes with varying geometries and contraction rates was conducted across a wide range of flow rates (1.136–69.71 L/s).

The experimental discharge coefficient ($C_{d,Exp}$) values showed excellent agreement with theoretical predictions ($C_{d,Th}$), with a maximum deviation of only 0.185%.

The approximate equation for C_d , valid for the wide range $0.05 \leq M_1 \leq 0.95$, was shown to reliably predict the discharge coefficient with minimal deviations.

Device Performance

The modified H-Flume demonstrated high accuracy for both high and low flow rates, attributed to the incorporation of the vertical V-notch.

The V-notch design raised upstream water levels, allowing for precise depth readings and reliable stage-discharge relationships.

The device's semi-modular nature was confirmed, with the flow rate depending on both the geometric characteristics of the flume and the upstream flow depth.

Practical Insights

The theoretical and experimental results validated the modified H-Flume as a controlled device with significant improvements over the original H-Flume.

The study provided guidelines for optimal device dimensions, ensuring negligible pressure drops and enabling critical flow conditions at the V-notch.

The approximate equations for $h_1^*(M_1)$ and $C_d(M_1)$ simplify field calculations without compromising accuracy, making the device practical for widespread use.

Accuracy Metrics

The explicit approximate relationship for $h_1^*(M_1)$ caused a maximum deviation of 0.094%, resulting in a maximum deviation of 0.235% in $C_d(M_1)$ calculations.

Added to the appendix, a more accurate, albeit cumbersome, explicit equation for $h_1^*(M_1)$ reduced deviations to 0.00185% for h_1^* and 0.00463% for C_d .

Is Adopting the Modified H-Flume a Wise Idea?

Yes, adopting the modified H-Flume appears to be a justified and wise decision, given that experimental studies have not identified the drawbacks observed in traditional designs. The strictly triangular vertical terminal section eliminates instabilities and improves discharge accuracy. It offers simpler theoretical modeling, better structural efficiency, and smoother flow transitions. While further field studies may be required, the absence of observed drawbacks makes it a highly promising innovation in flow measurement.

Comparison: Traditional vs. Modified H-Flume

Criteria	Traditional H-Flume (Inclined Trapezoidal outlet)	Modified H-Flume (Vertical Triangular outlet)
1 Flow stability	Moderate, may experience turbulence	High, smooth and predictable flow
2 Measurement accuracy	Good but affected by contraction inconsistencies	Very high, ensures well-defined critical section
3 Theoretical modeling	Requires additional empirical corrections	Aligns well with standard weir equations
4 Fabrication simplicity	More complex due to trapezoidal shape	Simpler due to strictly triangular shape
5 Structural efficiency	Stable, but material use is slightly higher	Optimized, potentially reducing material use
6 Sensitivity to flow variations	Lower sensitivity, suitable for a wider range of flows	Higher sensitivity, requires precise measurements
6 Need for empirical corrections	Requires adjustments for different flow conditions	Minimal, as it follows standard theoretical equations

Declaration of competing interest

The authors declare that they have no known competing financial interests or personal relationships that could have appeared to influence the work reported in this paper.

REFERENCES

ACHOUR B. (1989). Jump flow meter in a triangular cross-section without weir, *Journal of Hydraulic Research (In French)*, Vol. 27, Issue 2, pp. 205-214.

ACHOUR B., BOUZIANE M.T., NEBBAR M.L. (2003). Triangular broad crested flowmeter in a rectangular channel, *Larhyss Journal*, No 2, pp. 7-43. (In French)

ACHOUR B., AMARA L. (2020). Discussion of "discharge coefficient of shaft spillway under small heads, by GOURYEV A.P., BRAKENI A., BEGLAROVA E.C.", *Larhyss Journal*, No 43, pp. 7-11.

ACHOUR B., AMARA L. (2021a). Discharge coefficient for a triangular notch weir-theory and experimental analysis, *Larhyss Journal*, No 46, pp. 7-19.

ACHOUR B., AMARA L. (2021b). Theoretical discharge coefficient relationship for contracted and suppressed rectangular weirs, *Larhyss Journal*, No 45, pp. 165-182.

- ACHOUR B., AMARA L. (2021c). Discharge coefficient of a parabolic weir, theory and experimental analysis, *Larhyss Journal*, No 46, pp. 77-88.
- ACHOUR B., AMARA L. (2021d). Theoretical approach to stage-discharge relationship for a circular sharp-crested weir, *Larhyss Journal*, No 46, pp. 101-113.
- ACHOUR B., AMARA L. (2021e). Theoretical discharge coefficient relationship for a contracted triangular notch weir, experimental analysis for the special case of the 90-degree V-notch, *Larhyss Journal*, No 46, pp. 89-100.
- ACHOUR B., AMARA L. (2021f). Discharge measurement in a rectangular open-channel using a sharp-edged width constriction - theory and experimental validation, *Larhyss Journal*, No 45, pp. 141-163.
- ACHOUR B., AMARA L., MEHTA D. (2022a). Control of the hydraulic jump by a thin-crested sill in a rectangular channel, new experimental considerations, *Larhyss Journal*, No 50, pp. 31-48.
- ACHOUR B., AMARA L. (2022b). Triangular broad crested weir, theory and experiment, *Larhyss Journal*, No 49, pp. 37-66.
- ACHOUR B., AMARA L., MEHTA D., BALAGANESAN P. (2022c). Compactness of Hydraulic Jump Rectangular Stilling Basins Using a Broad-Crested Sill, *Larhyss Journal*, No 51, pp. 31-41.
- ACHOUR B., AMARA L., MEHTA D. (2022d). New theoretical considerations on the gradually varied flow in a triangular channel, *Larhyss Journal*, No 50, pp. 7-29.
- ACHOUR B., AMARA L. (2022e). Rectangular broad-crested flow meter with lateral contraction - theory and experiment, *Larhyss Journal*, No 49, pp. 85-122.
- ACHOUR B., AMARA L. (2022f). Accurate discharge coefficient relationship for the Crump weir, *Larhyss Journal*, No 52, pp. 93-115.
- ACHOUR B., AMARA L. (2023). Control of the hydraulic Jump by a broad-crested sill in a rectangular channel - new theory and experiment, *Larhyss journal*, No 54, pp.145-174.
- ACHOUR B., DE LAPRAY G. (2023). Curved Wall Triangular Flume (CWTF), Design, Theory, and Experiment, *Larhyss Journal*, No 56, pp. 139-178.
- ACHOUR B., AMARA L. (2023). The 2A triangular weir, Design, Theory and Experiment, *Larhyss Journal*, No 55, pp. 191-213.
- ACHOUR B., AMARA L., KULKARNI K.H. (2024). Modified Montana Flume (MMF), *Larhyss Journal*, No 60, pp. 55-85.
- ACHOUR B., MEHTA D., AZAMATHULLA H.M. (2024). A new trapezoidal flume for open channel flow measurement - design, theory, and experiment, *Larhyss Journal*, No 59, pp. 157-179.

- AFBLB. Financial Agency of the Loire and Brittany Basin. (1970). Book of special requirements for the production and approval of devices for measuring the flow of effluents. (In French)
- BAZIN H. (1898). New experiments on Weir flow, Dunod Editions, Paris, France. (In French).
- BOS M.G. (1989). Discharge measurement structure, 3rd Edition, Publication 20, International Institute for Land Reclamation and Improvement, Wageningen, Netherlands.
- BOS M.G. (1976). Discharge measurement structures, hydraulic laboratory, Wageningen, The Netherlands, Report 4, May.
- BRAKENSIEKD., OSBORN H., RAWLS W. (1979). Field manual for research in agricultural hydrology, agriculture handbook No 224, United Department of Agriculture, February, USA.
- BRANDES D., BARLOW W.T. (2012). New Method for Modeling Thin-Walled Orifice Flow Under Partially Submerged Conditions, Journal of Irrigation and Drainage Engineering, Vol.138, Issue 10, pp. 924-928.
- DE COURSEY D.E., BLANCHARD B.J. (1970). Flow analysis over large triangular weir, Proceeding ASCE, Journal of Hydraulics Division, Vol. 96, HY7, pp. 1435-1454.
- FARZAD A., VATANKHAH A.R. (2023). Experimental study of simple flumes with trapezoidal contraction, Flow Measurement and Instrumentation, Vol. 90, Paper ID 102328.
- GWINN W., PARSONS D. (1976). Discharge Equations for HS, H, and HL Flumes, Journal of the Hydraulics Division, Vol. 102, No 1.
- GWINN W. (1984). Chute Entrances for HS, H, and HL Flumes, Journal of Hydraulic Engineering, May.
- HAGER W.H. (1986). Discharge Measurement Structures, Communication 1, Department of Civil Engineering, Federal Polytechnic School of Lausanne, Switzerland. (In French)
- KINDSVATER C.E., CARTER R.W. (1957). Discharge characteristics of rectangular thin-plate weirs, Proceeding ASCE, Journal of Hydraulics Division, Vol. 83, HY6, pp.1453/1-6.
- KULKARNI K.H., HINGE G.A. (2021). Performance enhancement in discharge measurement by compound broad crested weir with additive manufacturing, Larhyss Journal, No 48, pp. 169-188.
- KULKARNI K.H., HINGE G.A. (2023). An energy perspective of composite broad crested weir for measuring accurate discharge, Larhyss Journal, No 54, pp. 85-106.

- LANGHAAR H.L. (1962). *Dimensional Analysis and Theory of Models*, Wiley and Sons Inc.
- OPEN CHANNEL FLOW. (2024). *Brochures, Flow Tables, Instructions for Flumes, Manholes, Shelters, and Weirs*, Atlanta, USA. Website accessible at <https://www.openchannelflow.com/support/downloads-center>
- PARSHALL R.L. (1936). The improved Venturi flumes, *Transaction, ASCE*, Vol. 89, pp. 841–880.
- SIA (Swiss Society of Engineers and Architects) (1936). *Contribution to the study of gauging methods*, Bulletin 18, Schweizer Wasserforschung, Bern, Switzerland. (In French).
- VATANKHAH A.R., BIJANKHAN M. (2013). Discussion of New Method for Modeling Thin-Walled Orifice Flow Under Partially Submerged Conditions, *Journal of Irrigation and Drainage Engineering*, Vol.139, Issue 9, pp. 789-793.
- ZUIKOV A.L. (2017). Hydraulics of the classical Crump weir water gauge, *Power Technology and Engineering*, Vol. 50, Issue 6, pp. 50-59

APPENDIX

Let us recall the non-linear implicit Eq. (16) governing the relative upstream depth h_1^* , from which the subsequent discharge coefficient relationship is based on:

$$h_1^{*5} - \frac{5}{4}h_1^{*4} + \frac{1}{4}M_1^2 = 0 \tag{A1}$$

The objective is to derive an approximate closed-form solution for this implicit algebraic equation in order to obtain explicitly h_1^* as a function of the dimensionless parameter M_1 . For that, let us consider the zeroth-order solution given by a quarter of an ellipse of equation:

$$\Psi = \frac{1}{4}\sqrt{1 - M_1^2} + 1 \tag{A2}$$

Introducing a second-order perturbation solution in Eq. (A1) around the zeroth-order solution (Eq. A2), yields the following:

$$\Psi^5 - \frac{5}{4}\Psi^4 + \frac{1}{4}M_1^2 + 5(\Psi^4 - \Psi^3)(h_1^* - \Psi) + \left(10\Psi^3 - \frac{15}{2}\Psi^2\right)(h_1^* - \Psi)^2 = 0 \tag{A3}$$

Eq. (A3) is quadratic in h_1^* and the relevant solution root is given as follows:

$$h_1^* = \frac{30\Psi^3 - 20\Psi^2 + \sqrt{-60\Psi^6 + 120\Psi^5 - 50\Psi^4 - 40M_1^2\Psi + 30M_1^2}}{40\Psi^2 - 30\Psi} \tag{A4}$$

Eq. (A4) along with Eq. (A2) give a closed-form approximate solution to the non-linear Eq. (A1) involved in the theoretical discharge coefficient governed by Eq. (22). It is worth mentioning that the maximum deviation from the true solution, expressed by Eq. (A4), is only 0.00185% in the whole range of M_1 , i.e. $0 \leq M_1 \leq 1$. Consequently, this causes a maximum deviation of only 0.0046% on the C_d discharge coefficient calculation, and as much on the calculation of the flow rate Q .

The following Table reports the distribution of the deviations caused by the use of Eq. (A4) as a function of M_1 , instead of using the exact implicit Eq. (A1). As can be seen, the deviations are extremely small.

M_1	h_1^* (Eq. A4)	Deviation (%)
1	1	0.0E+00
0.999	1.01394501	1.49E-04
0.99	1.0427712	9.02E-04
0.95	1.09041047	1.85E-03
0.9	1.12242794	1.71E-03
0.85	1.14487504	1.33E-03
0.8	1.16235525	9.59E-04
0.75	1.17664131	6.62E-04

0.7	1.18863644	4.40E-04
0.65	1.19887302	2.82E-04
0.6	1.20769464	1.74E-04
0.55	1.21533713	1.03E-04
0.5	1.22196966	5.76E-05
0.45	1.22771747	3.04E-05
0.4	1.23267551	1.49E-05
0.35	1.23691688	6.66E-06
0.3	1.24049841	2.63E-06
0.25	1.24346439	8.76E-07
0.2	1.24584914	2.33E-07
0.15	1.24767881	6.47E-05
0.1	1.24897263	9.48E-09
0.05	1.24974379	4.70E-10
0	1.25	0.0E+00
